NASA CR-134761

DESIGN, CONSTRUCTION AND EVALUATION OF A 12.045 GHz, 2.0 KW-CW PERMANENT-MAGNET FOCUSED KLYSTRON AMPLIFIER

by J. M. Nishida

VARIAN ASSOCIATES

prepared for
NATIONAL AERONAUTICS AND SPACE ADMINISTRATION

NASA Lewis Research Center
Contract NAS3-14393

1. Report No.	2. Government Accession No.	3. Recipient's Catalog No.
NASA CR-134761		

4. Title and Subtitle	5. Report Date
Design, Construction and Evaluation of a 12.045 GHz, 2.0 kW-cw Permanent-Magnet Focused Klystron Amplifier	February 1975
	6. Performing Organization Code
7. Author(s)	8. Performing Organization Report No.
9. Performing Organization Name and Address Varian Associates 611 Hansen Way Palo Alto, California 94303	10. Work Unit No.
	11. Contract or Grant No. NAS3-14393
	13. Type of Report and Period Covered Contractor Final Report
12. Sponsoring Agency Name and Address National Aeronautics and Space Administration Washington, D.C. 20546	14. Sponsoring Agency Code

15. Supplementary Notes

Project Manager, F. Kavanagh, NASA Lewis Research Center, Cleveland, Ohio

16. Abstract

This report describes an analytical and experimental program to demonstrate the technical feasibility of a lightweight, high-efficiency, 1 - 2 kW cw, permanent magnet focused klystron operating at 12.0 GHz.

The design is based on use of a samarium-cobalt permanent magnet for focusing of the electron beam and choice of the most optimum parameters for maximum efficiency. A filter-loaded output circuit is used for the required bandwidth.

The design incorporates a collector which is demountable from the tube to facilitate multistage depressed collector experiments, permitting replacement with a NASA-designed axisymmetric, electrostatic collector for linear beam microwave tubes.

A further requirement is that the focusing field between the last interaction gap and the collector decay in a prescribed manner referred to as "adiabatic expansion."

17. Key Words (Selected by Author(s))	18. Distribution Statement
samarium-cobalt permanent magnet axisymmetric electrostatic collector adiabatic expansion	Unclassified - unlimited

19. Security Classif. (of this report)	20. Security Classif. (of this page)	21. No. of Pages	22. Price*
Unclassified	Unclassified	51	$3.00

*For sale by the Clearinghouse for Federal Scientific and Technical Information, Springfield, Virginia 22151.

FOREWORD

The work described herein was done by Varian Associates, Palo Alto Tube Division under NASA Contract NAS3-14393 with the author as the principal investigator.

Others who have contributed significantly to the program are Mr. E. L. Lien, Mr. G. V. Miram and Mr. A. E. Berwick.

Mr. F. Kavanagh of the NASA-Lewis Research Center was the Project Manager.

ABSTRACT

This report describes an analytical and experimental program to demonstrate the technical feasibility of a lightweight, high-efficiency, 1 - 2 kW cw, permanent-magnet focused klystron operating at 12.0 GHz.

The design is based on use of a samarium-cobalt permanent magnet for focusing of the electron beam and choice of the most optimum parameters for maximum efficiency. A filter-loaded output circuit is used for the required bandwidth.

The design incorporates a collector which is demountable from the tube to facilitate multistage depressed collector experiments, permitting replacement with a NASA-designed axisymmetric, electrostatic collector for linear beam microwave tubes.

A further requirement is that the focusing field between the last interaction gap and the collector decay in a prescribed manner referred to as "adiabatic expansion."

TABLE OF CONTENTS

LIST OF ILLUSTRATIONS

LIST OF ILLUSTRATIONS (Cont.)

LIST OF TABLES

1. SUMMARY

A theoretical design for a permanent-magnet focused klystron is described. The objective was to obtain 2.0 kW cw with 120 MHz bandwidth at 12.045 GHz and with 45% conversion efficiency.

Both large- and small-signal programs were employed to analyze the design and to select design parameters for maximum conversion efficiency.

One klystron was fabricated to verify the analytical design.

The first experimental tube was Brillouin focused with a samarium-cobalt permanent-magnet focusing structure. A five-cavity design with a filter-loaded output cavity was used for the gain bandwidth requirements.

Test results from the one tube fabricated showed the design to have poor beam transmission due to insufficient magnetic field for rf operation.

The use of an auxiliary solenoid to increase the focusing field improves performance, and indicates more field is needed.

The permanent magnet is made up of 52 segments arranged in annular configuration, with a radial direction of magnetization.

2. INTRODUCTION

This report describes a development and experimental program for a lightweight, broadband klystron to be used for operation with a NASA-designed multistage depressed collector.[1, 2] One tube and ten demountable guns were to be delivered to Lewis Research Center.

The first task on the program was the development and analytic optimization of the design. This was followed by the physical design to achieve the characteristics selected. The third task was to construct and evaluate the selected design.

One tube was constructed and evaluated.

3. DESIGN APPROACH AND TRADEOFF CONSIDERATIONS

The basic design approach was to use a conventional five-cavity klystron rf circuit with drift lengths, drift tube diameters, beam diameters and gap coupling factors chosen to maximize conversion efficiency. The factors which influenced the initial choice of parameters are outlined in this section.

3.1 SUMMARY OF TUBE SPECIFICATIONS

The major klystron specifications are summarized in Table I. Those specifications which most directly affect the choice of design parameters are frequency, gain, power and efficiency.

TABLE I

MAJOR KLYSTRON SPECIFICATIONS

Electronic Conversion Efficiency	45% min
Center Frequency	12.045 GHz
Bandwidth	120 MHz
Rf Power Output	1.0 kW min
Power Gain	40 dB min
Design Life	2 years min
Phase Linearity $d^2\phi/d\omega^2$	$0.2°/MHz^2$
Noise Figure	40 dB max
Perveance	0.75×10^{-6} max
Beam Transmission at Saturation	95% min
Maximum Beam Voltage	16 kV
Demountable Electron Gun	

3.2 SUMMARY OF FOCUSING MAGNET SPECIFICATIONS

- Maximum field: 2000 gauss
- Length of focusing field: 7.62 cm
- Maximum leakage field into collector: +0.5%
- Field reversal in the collector region: Not allowed
- "Adiabatic Beam Expansion" from the last interaction gap into the collector
- Demountable collector
- Assembly to be bakeable to 250°C

3.3 INITIAL ELECTRICAL DESIGN

The selected beam power is 4.444 kW based on a 45% conversion efficiency and an output power of 2 kW. A low beam perveance is desirable to maximize efficiency; however, the length of the rf circuit increases with decreasing perveance, and the weight of the magnet increases as the cube of the length. In addition to these factors, small signal computer analysis shows that at least a 35% increase in the R/Q would be required, and even this would result in marginal gain-bandwidth.

Therefore, the maximum allowable perveance of 0.75×10^{-6} is the most suitable for this tube.

With the parameters chosen so far (i.e., beam power and perveance), the beam voltage will be 8.111 kV and the beam current is 0.548 A.

The normalized tunnel diameter predominantly affects the efficiency and the beam and gun designs. The minimum practical drift tube diameter is determined by the beam size, and since the cavity R/Q is also influenced by drift tube diameter, it is doubly important to minimize the diameter of both the beam and drift tube. Conversely, a lower limit on beam size is set by space-charge effects and by beam optics and focusing considerations. As the beam size is decreased, the required focusing field increases, and the magnet weight increases as the square of the focusing field. The required area convergence of the gun decreases with increasing tunnel diameter, while the conversion efficiency decreases rapidly when the normalized tunnel radius, γa, exceeds 0.90 radian.

The required bandwidth of 120 MHz and phase deviation specification dictate that the second and third buncher cavities be resistively loaded to increase the buncher section bandwidth. The required bandwidth also makes it necessary to use something other than a conventional output cavity. To achieve the necessary output circuit bandwidth, a filter-loaded output circuit is used.

The design approach taken was to make the drift tube diameter and the beam diameter larger in the buncher section and smaller in the output section. The larger tunnel and beam diameter allow the use of a lower convergence gun and a smaller magnet. This has only a minor effect on gain and bandwidth. The smaller tunnel and beam in the output section are necessary to maintain the conversion efficiency.

The remaining major design parameters are number and Q factors of cavities, interaction gap lengths, and intercavity gap lengths.

4. ANALYTICAL DESIGN

The analytical design procedure was based on several Varian computer programs which model electron trajectories and the rf interaction process in a klystron. These programs were used to refine the initial design; i.e., to ensure that the klystron would perform with proper gain and bandwidth, as well as to predict the efficiency. Because the programs are basically analytic rather than synthetic in nature, it was necessary, in order to synthesize a design, to compute a number of designs in order to systematically optimize a given parameter.

4.1 REVIEW OF ANALYTIC CAPABILITY

The main analytical tools used in this program were our small-signal and large-signal computer programs for klystron amplifiers, with computer programs and beam analyzers used for the electron gun and beam design.

The small-signal computer program is based on space-charge wave theory and is capable of predicting the small-signal gain and phase delay, and the first and second derivatives of the phase delay, as a function of operating frequency. The small-signal analyses were used in the selection of the number of cavities and for adjustment of the tuning and loaded Q factors of the resonators. The final adjustment of the tuning pattern, however, was done experimentally.

The large-signal computer program used in the tube analysis is based on a program developed at Cornell University, modified to account for the effect of the drift tube on the rf space charge forces.[3] This program has been capable of predicting the efficiency of klystron amplifiers within about 5 percentage points at the 50% efficiency level, and within about 10 percentage points at the 70% efficiency level. The large-signal program is used for comparison of the efficiency of different designs and for calculation of the optimum loading of the output resonator. No specific large-signal calculations were made for this tube design, but use was made of the general design concepts for selection of parameters derived in previous company-sponsored study programs.[4]

The gun design computer program solves the electron trajectories for arbitrary beam flow problems including space charge, axially-symmetric magnetic fields, relativistic effects (including the self-magnetic field of the beam) and the effects of thermal velocities. In addition to the design of electron guns, collector beam spread calculations may also be performed with this program.

Varian's beam tester thoroughly evaluates the performance of actual gun configurations. Salient features of this machine include a pinhole and split-collector arrangement which can be used to scan the beam in two transverse directions as well

as along the beam axis, a well-shielded solenoid so that measurements can be made with an applied focusing field, and an oil-free vacuum chamber.

4.2 SMALL-SIGNAL ANALYSIS

The initial small-signal analysis began by using assumed design parameters selected as feasible values from previous work on similar tubes. This was primarily a verification process to show that the basic tube specifications could be met with a five-cavity approach, and will not be discussed in detail. The next step was the actual design and cold test of the individual cavities, providing measured cavity characteristics for use in the small-signal computer calculations.

The chosen and measured parameters for the first tube are listed in Table II. These figures were used to compute the small-signal gain, bandwidth and phase response. The results of the final computations are shown in Figure 1, which is the actual computer terminal printout.

The small-signal gain is 47.7 dB, as shown in Figure 2. The bandwidth of Channel 1 is just shy of the required 40 MHz and the bandwidth of Channel 4 is slightly over 40 MHz. A slight tuning adjustment would give the necessary bandwidth on Channel A. The cavity tuning scheme is given under F (GHz) (Figure 1). Channels A and B are to be used as guard band and the gain does not drop below 3 dB. Figure 3 is the calculated $d^2\phi(\omega)/d\omega^2$ as a function of frequency. The specification of a maximum second-order phase deviation of $0.2°/MHz^2$ is not met in Channel 1, but is within specification in Channel 2. To reduce the second order phase deviation in Channel 1 will require more loading in the cavities; however, this in turn will reduce the gain.

4.3 ELECTRON GUN AND BEAM DESIGN

The electron gun is of the type commonly referred to as Brillouin focused. The object of the design is to obtain a beam which is laminar and with minimum scalloping, and maintained in equilibrium with a magnetic focusing field of the Brillouin value. Since experience has shown that some difficulty may arise in maintaining adequate focusing under rf conditions, the design approach is to have the beam enter the magnetic field at the Brillouin value, then gradually increase the focusing field to 1.5 times the Brillouin field at the last interaction gap.

The gun used on the tube is a modification of an existing gun. The modifications are made and the results checked in the beam analyzer. After several trial runs in the beam analyzer, a suitable gun was finalized. Table III shows the major gun parameters.

TABLE II

FINAL DESIGN PARAMETERS

Frequency	12.045 GHz
Bandwidth	120 MHz
Beam Voltage	8.111 kV
Beam Current	0.548 A
Beam Perveance	0.75×10^{-6}
Beam Area Convergence	46:1
Cathode Loading	1.73 A/cm^2
Cathode Diameter	0.635 cm
Number of Cavities	5
R/Q Input Cavit	124
R/Q Second Cavity	124
R/Q Third Cavity	124
R/Q Fourth Cavity	105
R/Q Output Cavity	110
Normalized Length of Interaction Gaps	
1st Gap	1.02 radian
2nd Gap	1.02 radian
3rd Gap	1.02 radian
4th Gap	1.02 radian
Output Gap	0.69 radian
Normalized Tunnel Radius, γa	
Cavity Numbers 1, 2, 3	1.067 radian
Cavity Numbers 4 and 5	0.90 radian
Tunnel Diameter, Cavity 1, 2, 3	0.151 cm
Cavity 4 and 5	0.127 cm

TABLE II (Cont.)

Beam-Filling Factor, b/a	
Cavity 1	0.62
Cavity 2	0.49
Cavity 3	0.43
Cavity 4	0.52
Cavity 5	0.55
Drift Lengths	
ℓ 1,2	1.27 cm
ℓ 2,3	1.27 cm
ℓ 3,4	1.00 cm
ℓ 4.5	0.635 cm
Normalized Drift Length	
$\beta_q \ell$ 1,2	1.27 radian
$\beta_q \ell$ 2,3	1.54 radian
$\beta_q \ell$ 3,4	1.12 radian
$\beta_q \ell$ 4,5	0.712 radian
Magnetic Focusing Field at the Last Interaction Gap	2000 gauss

GAIN-BANDWIDTH CALCULATIONS
V0= 8.1 KV G0= 6.7500E-05 MHO F0=12.0450 GHZ QE1= 200 W/W0=12.97

CAV	M+	M-	R/Q	Q	BQL	F(GHZ)
1	0.7216	0.7746	124	150	0.000	12.0330
2	0.6985	0.7669	124	450	1.278	11.9900
3	0.6935	0.7610	124	300	1.538	12.0900
4	0.7538	0.8112	105	713	1.114	12.1192
5	0.7916	0.8379	18000	1	.712	12.0450

F(GHZ)	DB GAIN	PHASE DEG	DP DEG	DP/DF DEG/MHZ	D2P DEG	D2P/DF2 DEG/MHZ↑2
11.9750	40.07	44.4	0.00	0.000	0.0000	0.0000
11.9800	42.81	58.9	14.49	2.899	5.1883	0.2075
11.9850	45.33	78.6	19.68	3.936	4.6649	0.1866
11.9900	47.06	102.9	24.35	4.869	0.4705	0.0188
11.9950	47.67	127.8	24.82	4.963	-3.7118	-0.1485
12.0000	47.49	148.9	21.11	4.221	-4.2171	-0.1687
12.0050	47.07	165.8	16.89	3.378	-2.8946	-0.1158
12.0100	46.68	179.8	13.99	2.799	-1.6343	-0.0654
12.0150	46.41	192.1	12.36	2.472	-0.8209	-0.0328
12.0200	46.24	203.6	11.54	2.308	-0.3706	-0.0148
12.0250	46.14	214.8	11.17	2.234	-0.1665	-0.0067
12.0300	46.08	225.8	11.00	2.200	-0.1165	-0.0047
12.0350	46.04	236.7	10.89	2.177	-0.1425	-0.0057
12.0400	45.99	247.4	10.74	2.148	-0.1750	-0.0070
12.0450	45.96	258.0	10.57	2.113	-0.1594	-0.0064
12.0500	45.96	268.4	10.41	2.082	-0.0605	-0.0024
12.0550	46.01	278.8	10.35	2.070	0.1401	0.0056
12.0600	46.14	289.3	10.49	2.098	0.4524	0.0181
12.0650	46.36	300.2	10.94	2.188	0.8801	0.0352
12.0700	46.67	312.0	11.82	2.364	1.4010	0.0560
12.0750	47.05	325.2	13.22	2.644	1.9059	0.0762
12.0800	47.42	340.4	15.13	3.025	2.1085	0.0843
12.0850	47.64	357.6	17.24	3.447	1.6200	0.0648
12.0900	47.56	376.5	18.86	3.771	0.4819	0.0193
12.0950	47.15	395.8	19.34	3.867	-0.4113	-0.0165
12.1000	46.54	414.7	18.93	3.785	-0.0026	-0.0001
12.1050	45.95	433.6	18.92	3.785	2.3535	0.0941
12.1100	45.57	454.9	21.28	4.255	7.0549	0.2822
12.1150	45.12	483.3	28.33	5.666	0.0000	0.0000

PROCESSING 4 UNITS

Figure 1. Computer Printout of Gain, Bandwidth and Phase

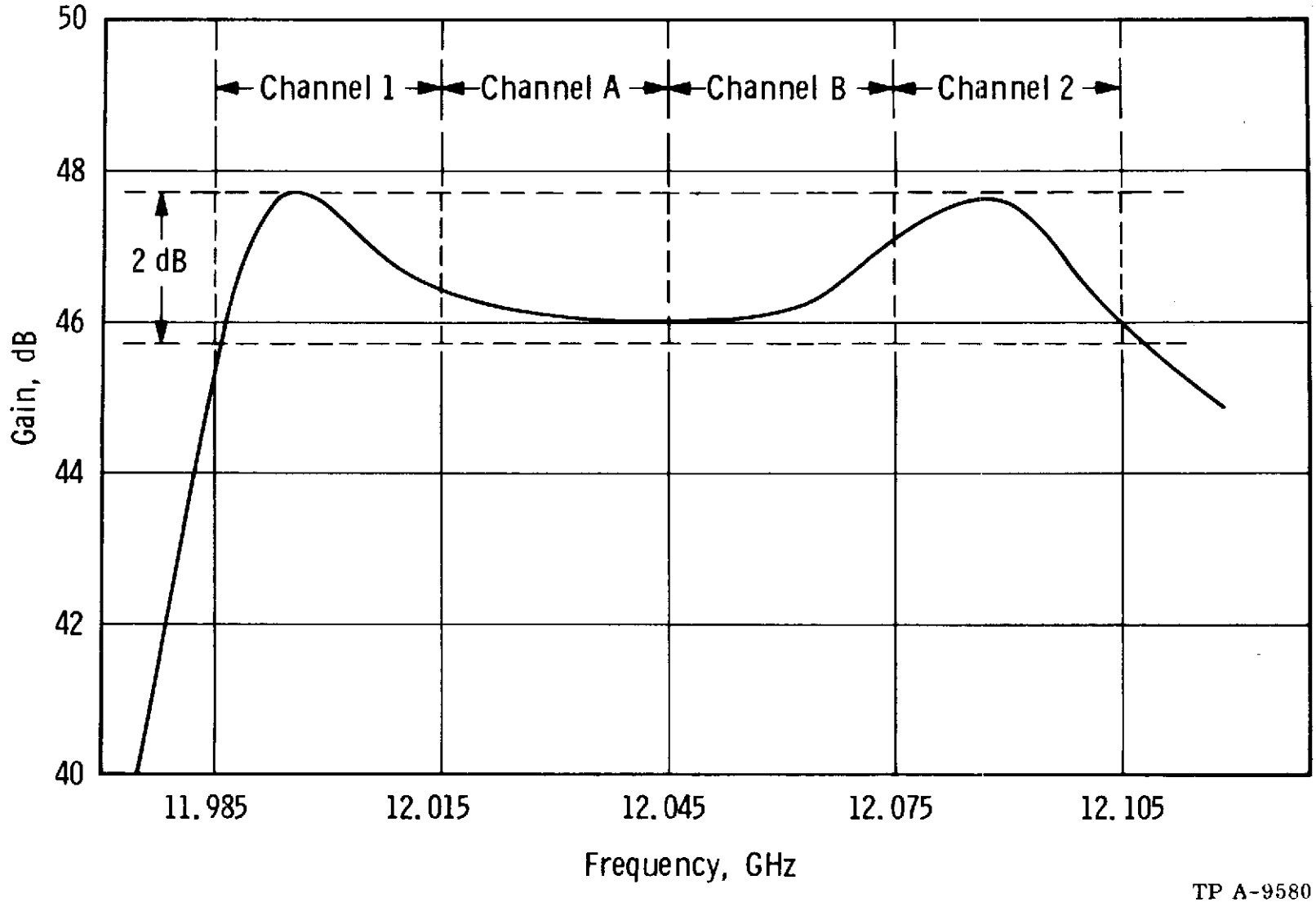

Figure 2. Computed Small Signal Gain as a Function of Frequency

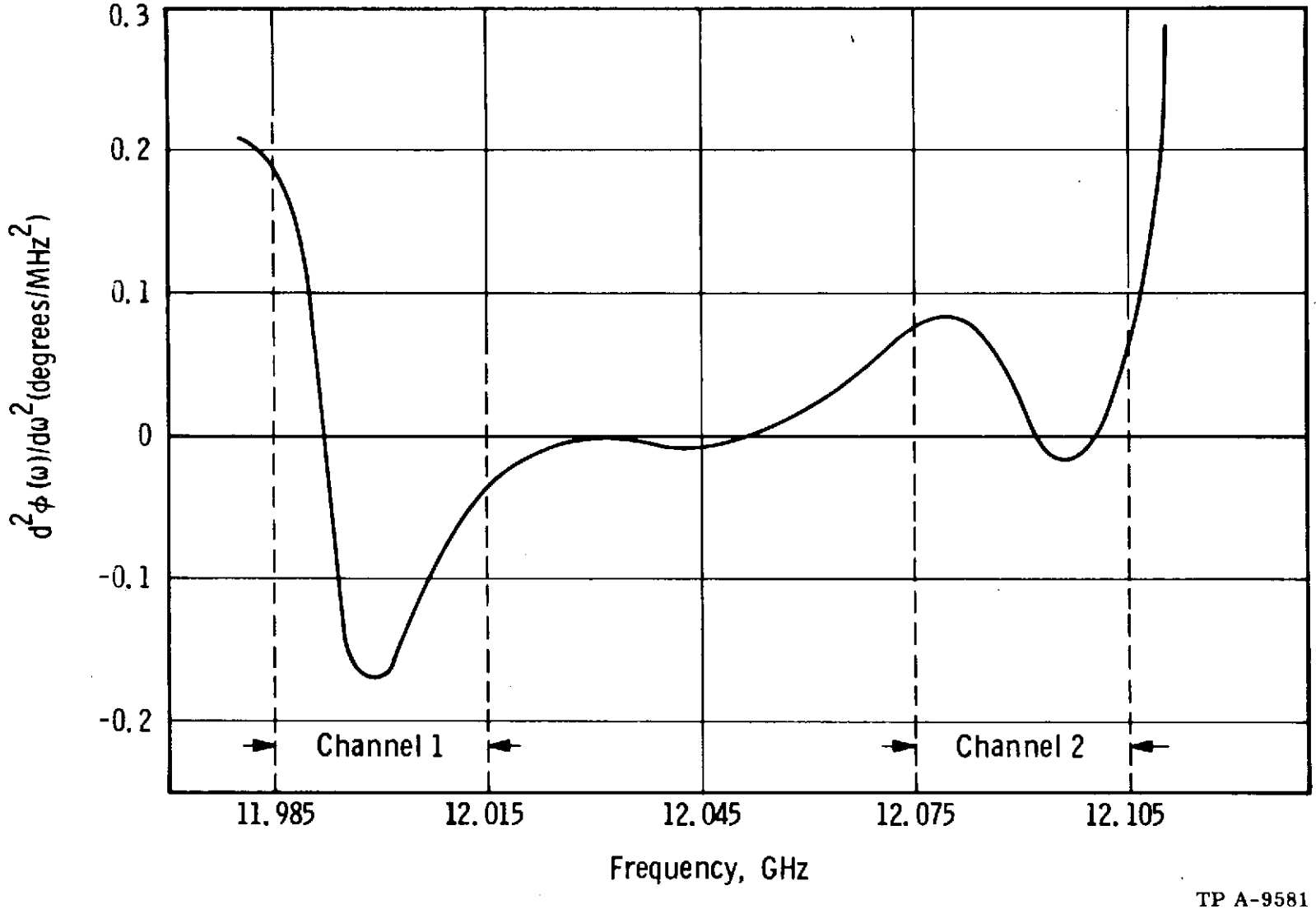

Figure 3. Calculated $d^2\phi(\omega)/d\omega^2$ as a Function of Frequency

TABLE III

GUN PARAMETERS

Cathode Diameter	0.635 cm (0.250 in)
Beam Diameter	0.094 cm (0.037 in)
Area Convergence	46:1
Perveance	0.75×10^{-6}

Figure 4 shows a sequence of cross sections of beam-current density as the beam proceeds downstream from the anode. The gun has been scaled up in size to a 1-inch diameter cathode in order to increase the accuracy of measurement in the beam analyzer.

Refer to Appendix A for a more detailed discussion on the operation of the beam analyzer.

4.4 PERMANENT-MAGNET FOCUSING DESIGN

The required focusing field as a function of axial distance from the cathode to the collector is governed by the requirements of (1) gun optics, (2) focusing field in the rf interaction region, and (3) the adiabatic expansion of the beam into the collector.

The basic magnetic circuit shown in Figure 5 consists of a ring-shaped samarium-cobalt magnet located in the gun end of the cylindrically-symmetric magnetic return path, a leakage shield over the gun end, and a floating polepiece in the beam expansion region.

The general approach is to analyze a trial magnetic circuit with a proprietary Varian computer program which solves Laplace's equation on a finite mesh for arbitrary closed-boundary conditions. The results of the computer solution are used to calculate the magnetic properties of the circuit, which are then compared with the required properties. Adjustments are made to the trial circuit and the analysis repeated until the desired properties are achieved.

A computer plot of the initial circuit is shown in Figure 6. The magnet itself is simulated by an electric potential drop along its length and the iron circuit by unipotential surfaces. The lines of constant flux are plotted by the computer and the axial magnetic field, calculated from the computer results, is also shown.

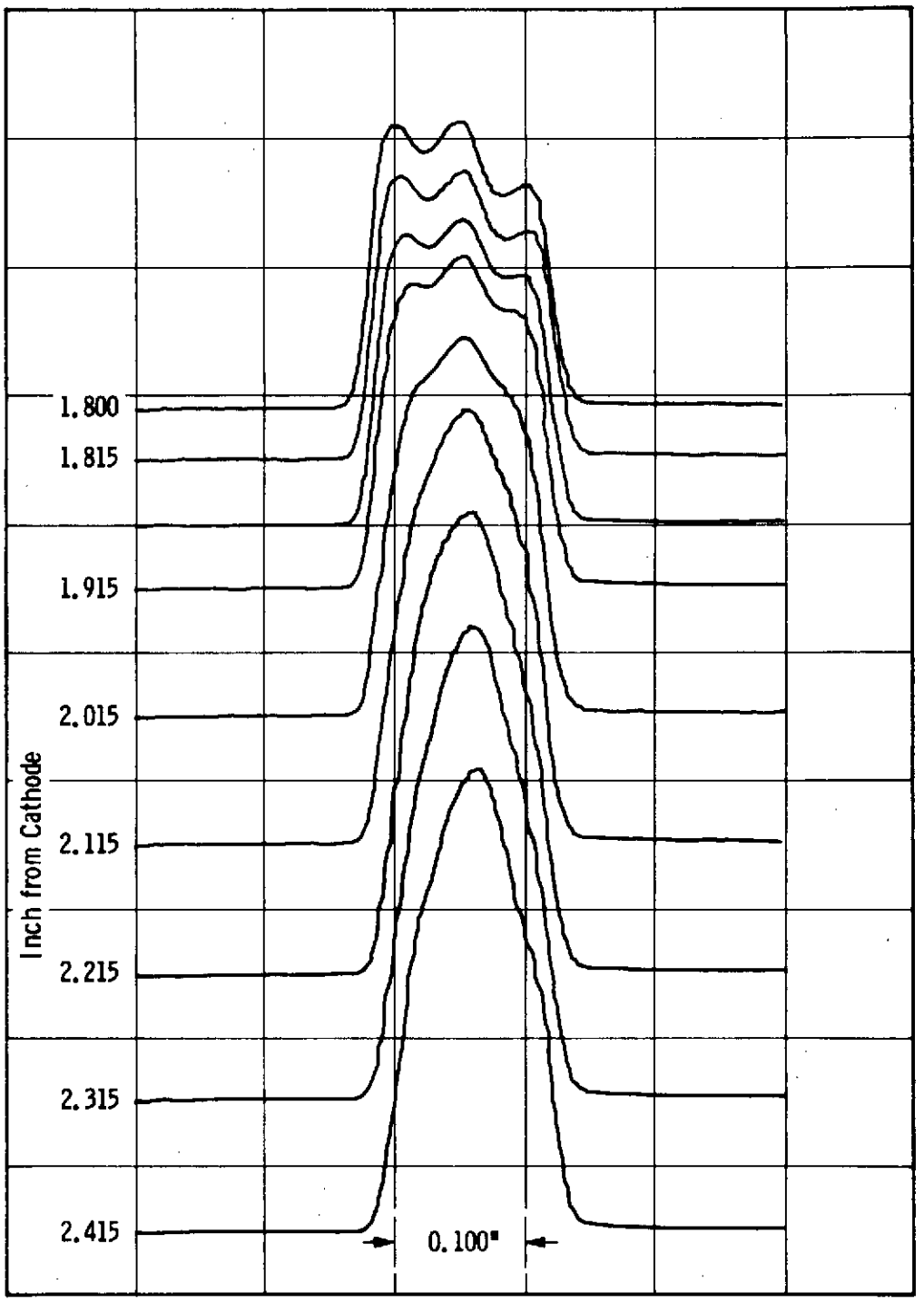

Figure 4. Beam Current Density vs Axial Distance from Cathode

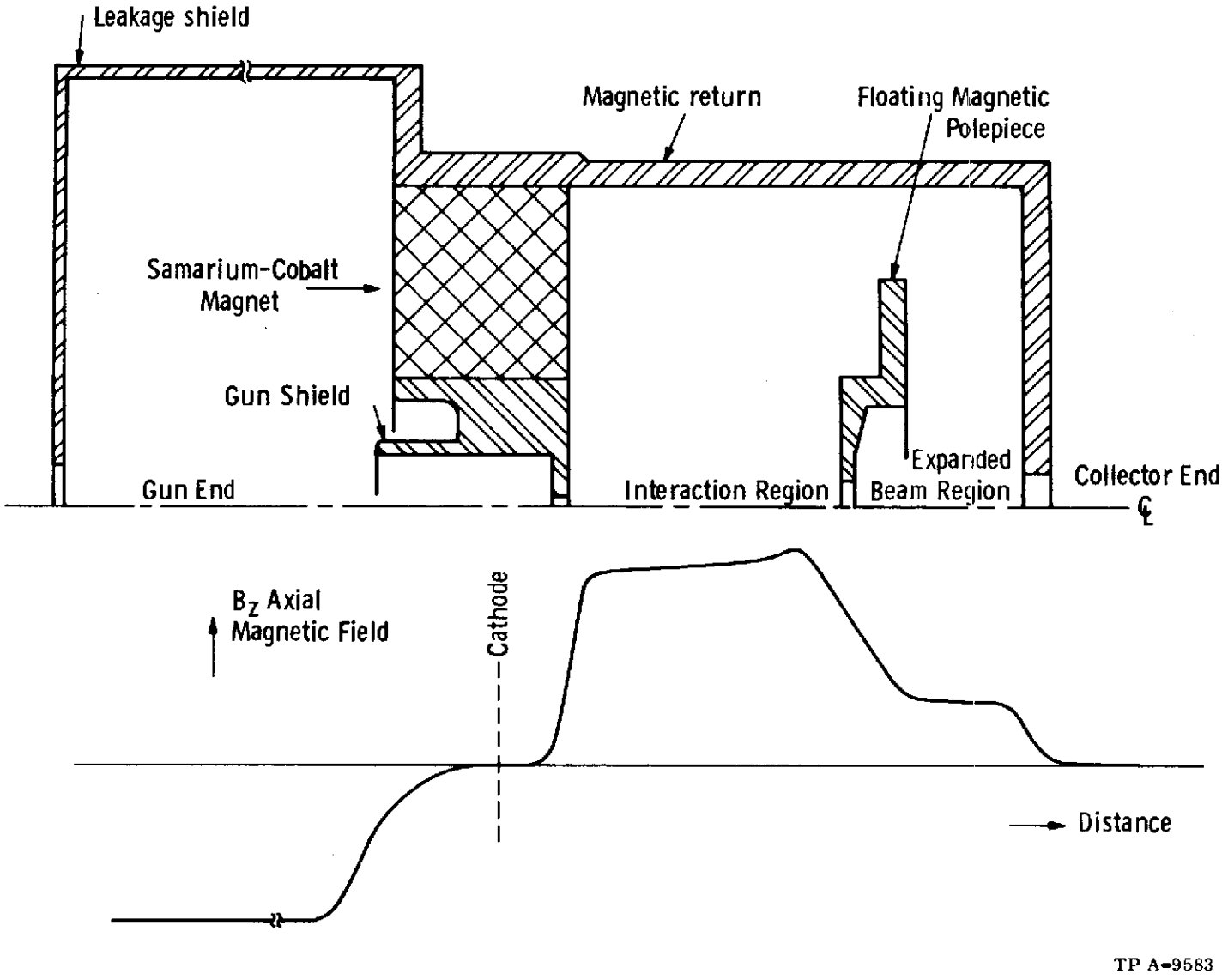

Figure 5. Proposed Magnetic Circuit Showing the Variation of the Axial Magnetic Field Along the Circuit

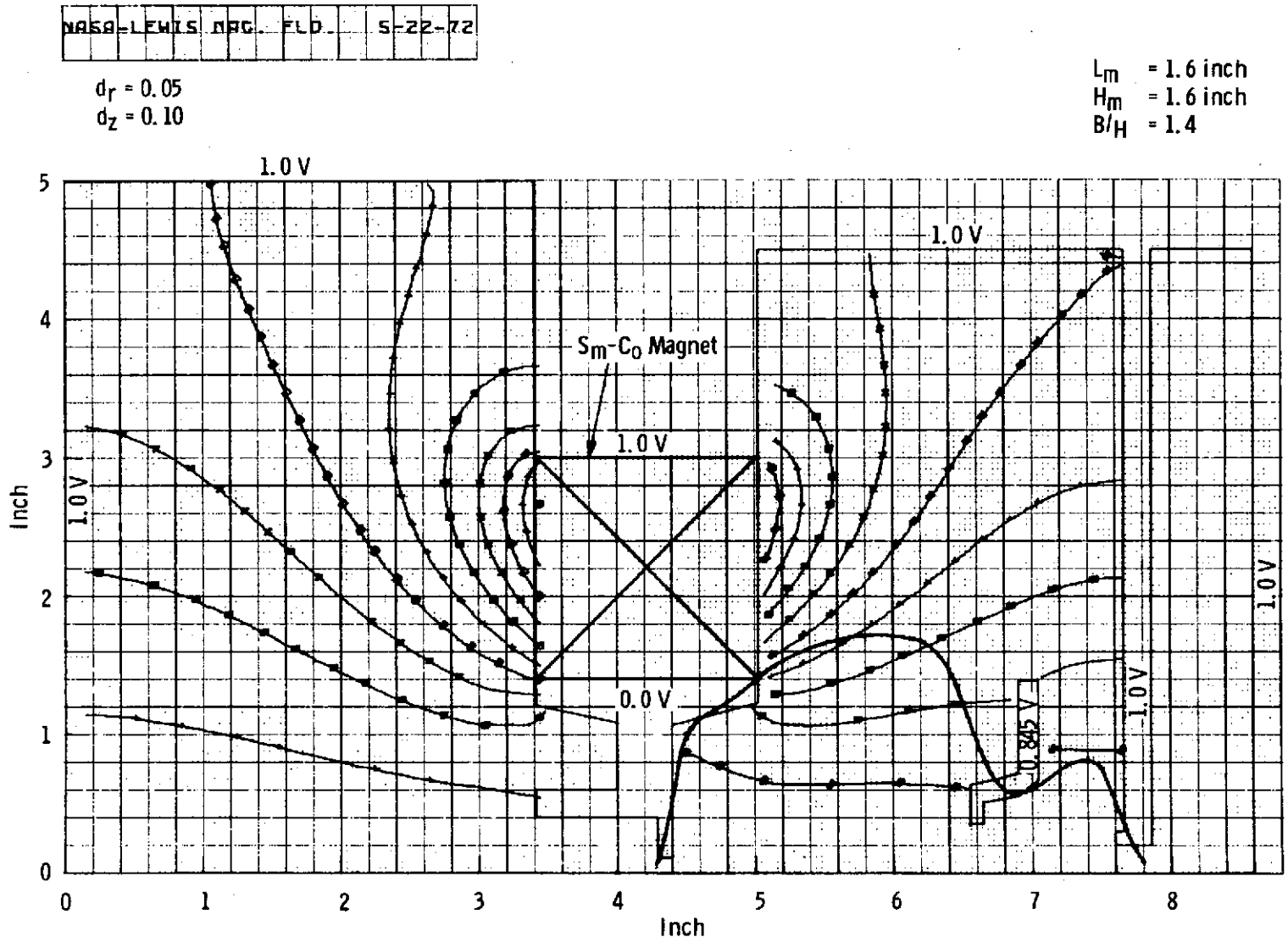

Figure 6. Computer Printout of Initial Magnet Design

The samarium-cobalt magnet has an ID of 7.11 cm (2.8 in), an OD of 15.24 cm (6.0 in), a thickness of 4.06 cm (1.6 in), and weighs 4.68 kg (10.3 lb). The maximum field is 2070 gauss. The shape and position of the floating polepiece gives approximately the required field shape for the beam expansion region. The final size and shape of the floating polepiece was determined experimentally on a half-scale model by varying the configuration, measuring the magnetic field, and then computing the beam trajectories on the computer program.

Figure 7 is an expanded detail of Figure 6 to show the location of the interaction gaps.

The operating point of the magnet is on a load line of 1.4 which is at the point of maximum energy product. Figure 8 is a plot of energy product vs load line, and shows little variation of the energy product as the load line varies between 1 and 2.

Figure 9 shows the demagnetization curves for the Varian-manufactured samarium-cobalt magnets for various stabilization temperatures. The design is based on a magnet stabilized at 300°C.

4.4.1 Experimental Results

A one-half scale model of the circuit shown in Figure 6 was constructed to check the computed design. Figure 10 shows the experimental vs computed data normalized to 100% Bz. Close agreement is shown in the rf interaction region and less field is shown in the beam expansion region. The reason for this is that the experimental circuit was made with a larger hole in the floating polepiece and exit magnetic shield because more space was needed in this area to fit the tube. The magnetic circuit is sketched in to show its relationship to the field.

The next task was to alter the collector and floating polepieces and compute the beam trajectory, then repeat the procedure until adiabatic beam expansion is achieved. The result is shown in Figure 11. The beam traverses the output gap with a diameter of 0.027 inch and gradually expands to 0.110 inch in a distance of 0.9 inch, remains constant for 0.3 inch, and then gradually expands into the collector region.

Using a value of 8.15 kV for the beam voltage and 2070 gauss for the magnetic field, the cyclotron wavelength is:

$$\lambda c = 264 \frac{VkV}{B \text{ gauss}} = 264 \frac{8.15}{2070} = 0.314 \text{ inch;}$$

therefore,

$$2\lambda c = 0.728 \text{ inch} .$$

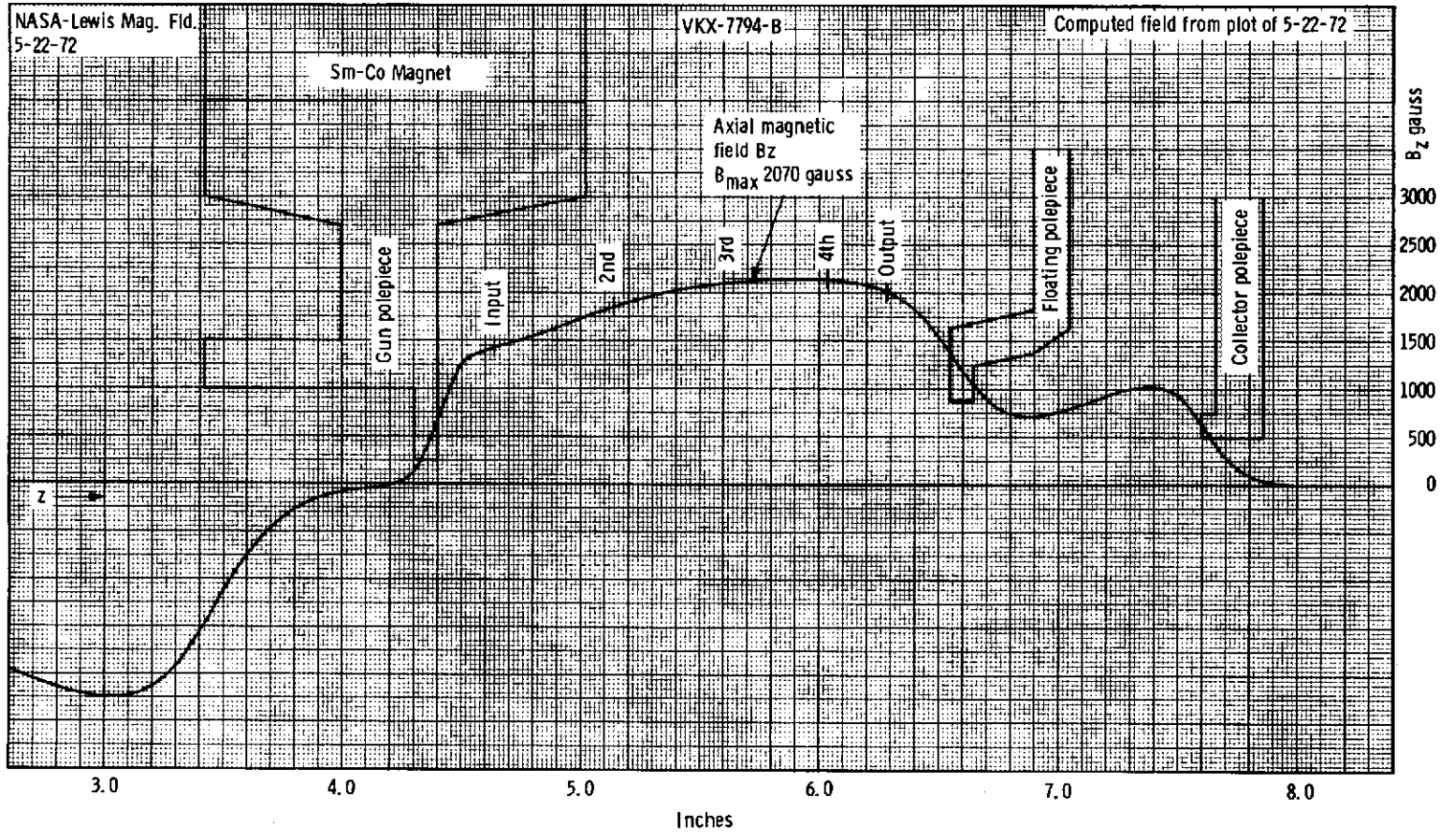

Figure 7. Expanded Detail of Figure 6

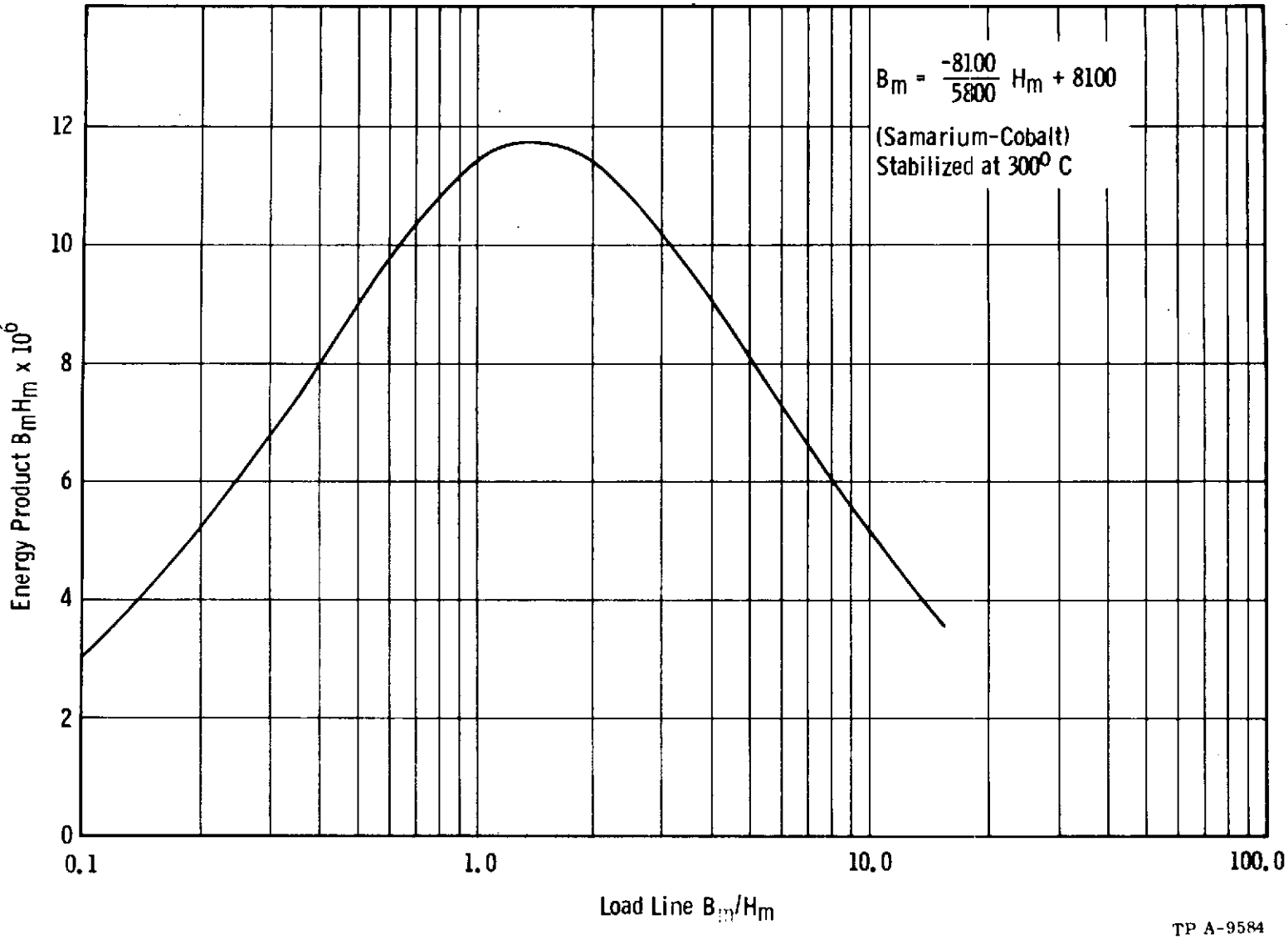

Figure 8. Energy Product vs Load Line

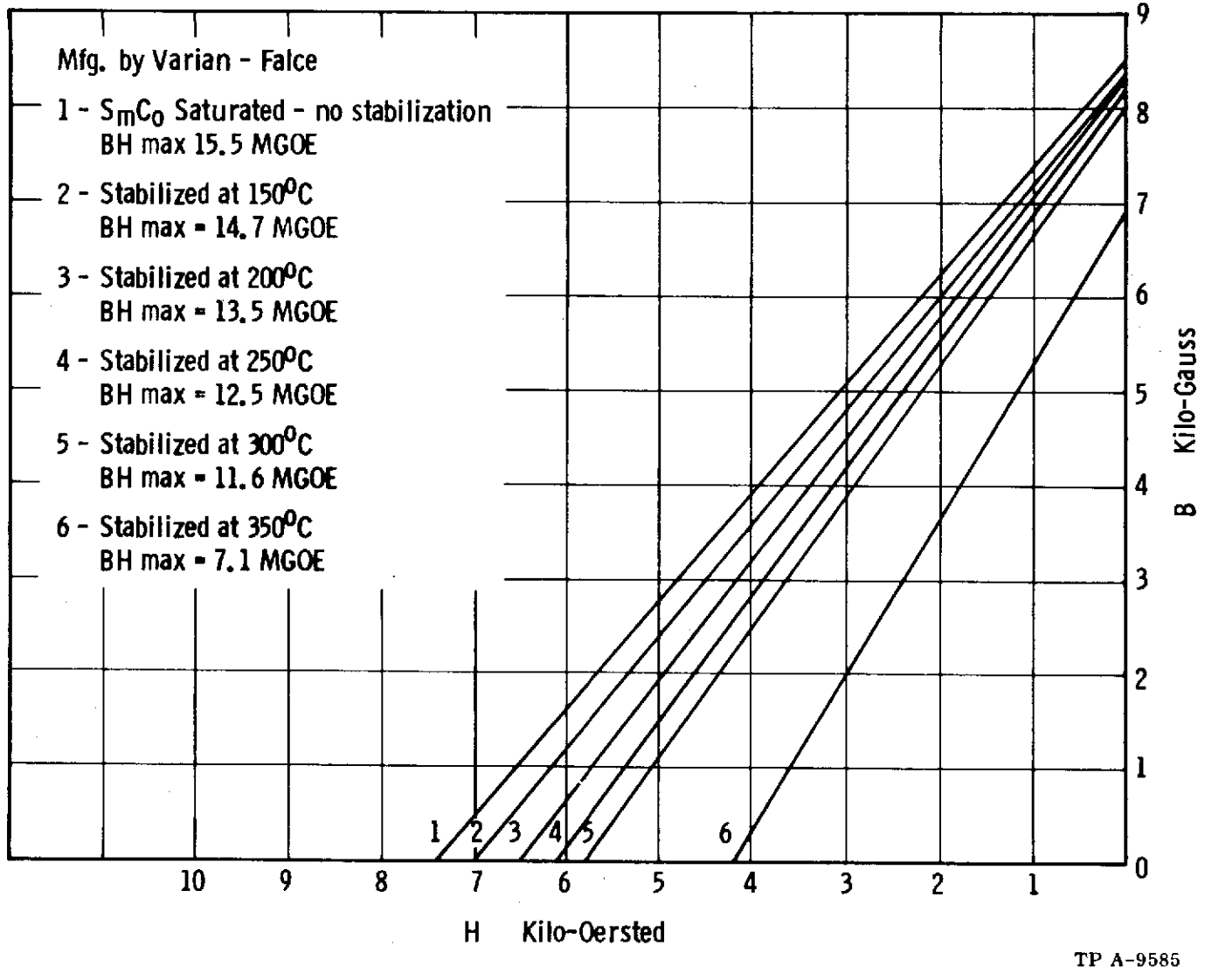

Figure 9. Demagnetization Curves for Varian-Manufactured SmCo Magnets

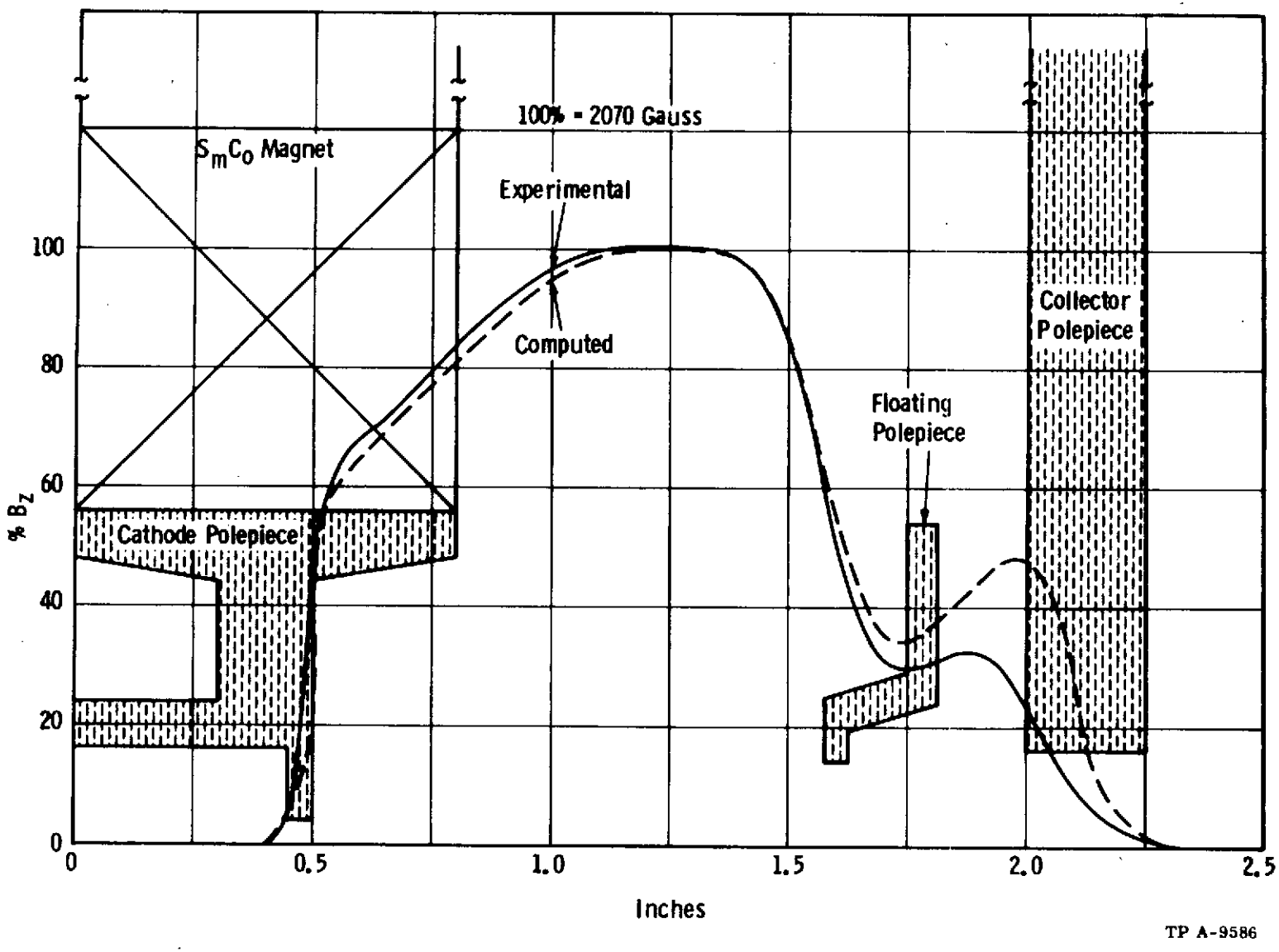

Figure 10. Experimental vs Computed Data Normalized to 100% B_z

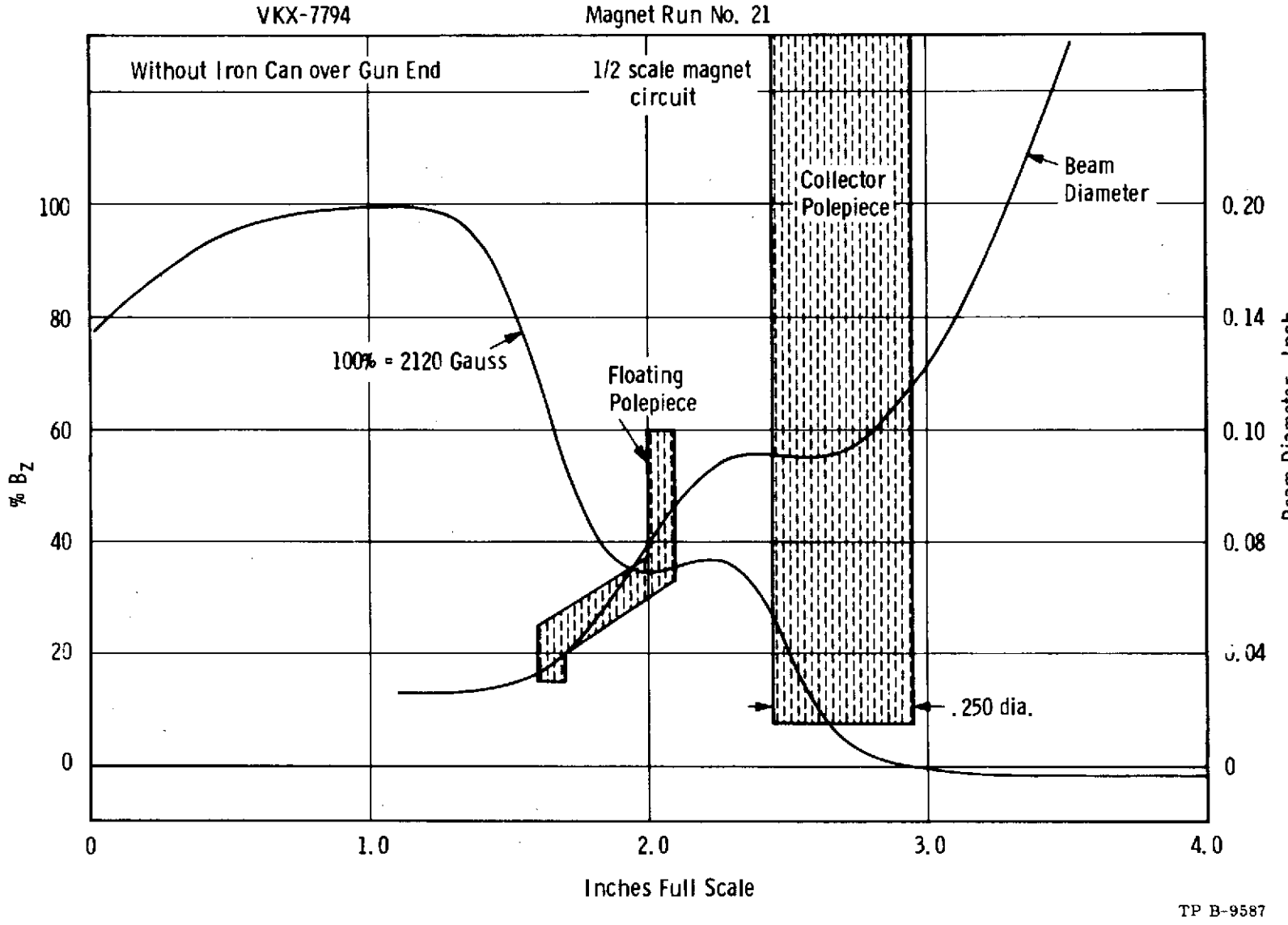

Figure 11. Magnetic Field and Beam Trajectory as a Function of Axial Distance

The length of the tapered field is 0.75 inch and meets the requirement that the tapered field must be greater than $2\lambda c$.

The tunnel diameter tapers out to 0.200 inch before entering the collector.

The electron beam is required to exit into a magnetically field-free collector. The maximum collector field at a position two exit hole diameters beyond the collector polepiece face must be less than 0.5% of the focusing field.

The collector polepiece configuration and the resulting measured magnetic field is shown in Figure 12.

This polepiece configuration produces a maximum collector field less than 0.5% of the focusing field. A large cylindrical shield around the gun end of the magnet must be used to prevent stray leakage fields from producing a negative field in the collector region. If this shield is not used, the collector field may be as high as -2%.

The next task was to examine in detail the magnetic field at the cathode. For Brillouin flow, there must be no field at the cathode. The initial design had a -1% field at the cathode; this was deemed to be excessive for good beam optics. Again by trial, the polepiece configuration around the cathode was modified for minimum field at the cathode. The final result is shown in Figure 13 and shows the field at the cathode to be -0.1%. This was judged to be close enough to zero to give proper gun performance.

4.5 COLLECTOR DESIGN

The collector is from an existing 10 kW klystron and easily handles the power level involved. The maximum power density is 3.15 kW/in^2.

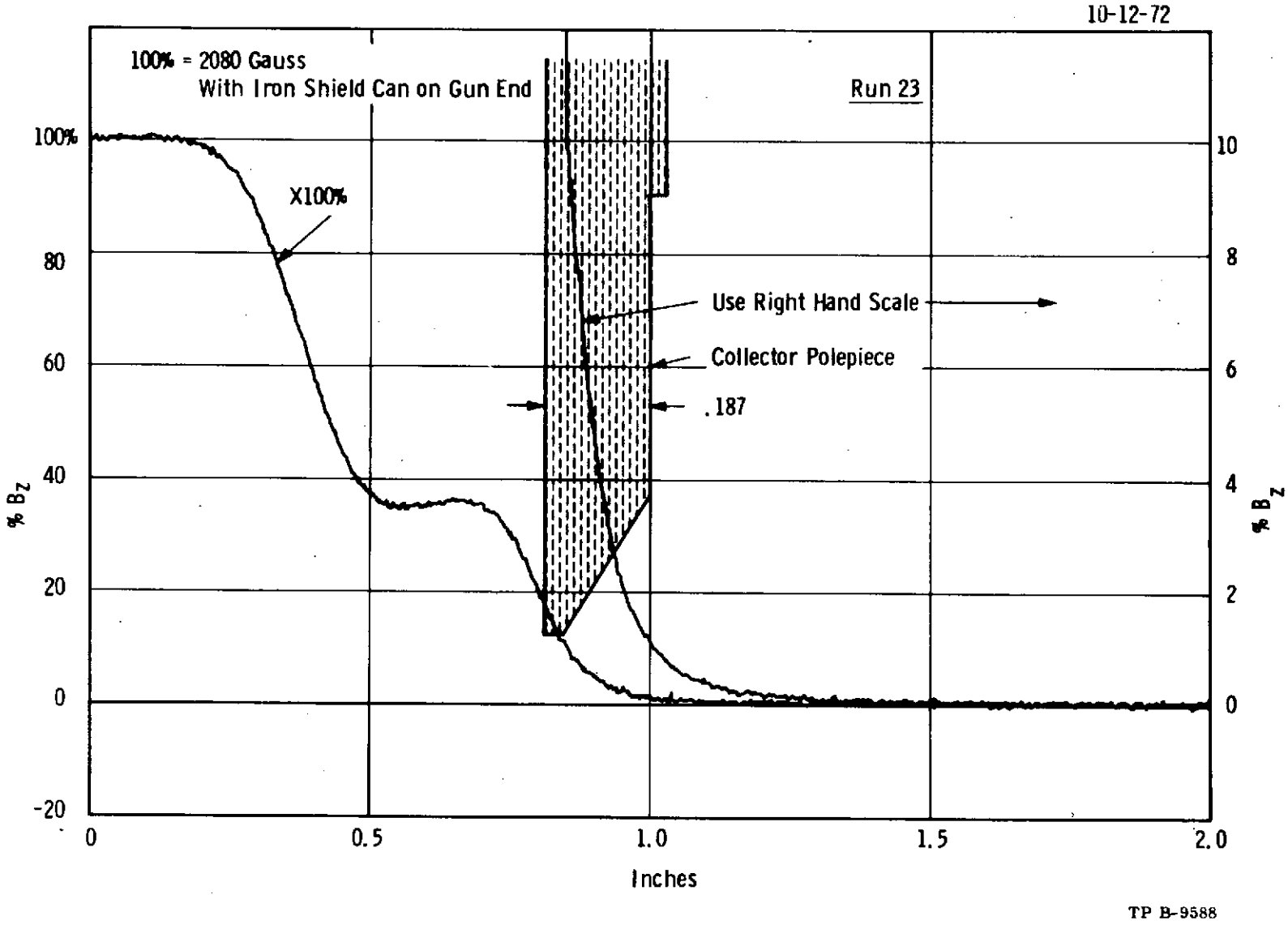

Figure 12. Leakage Magnetic Field Into the Collector Region vs Distance

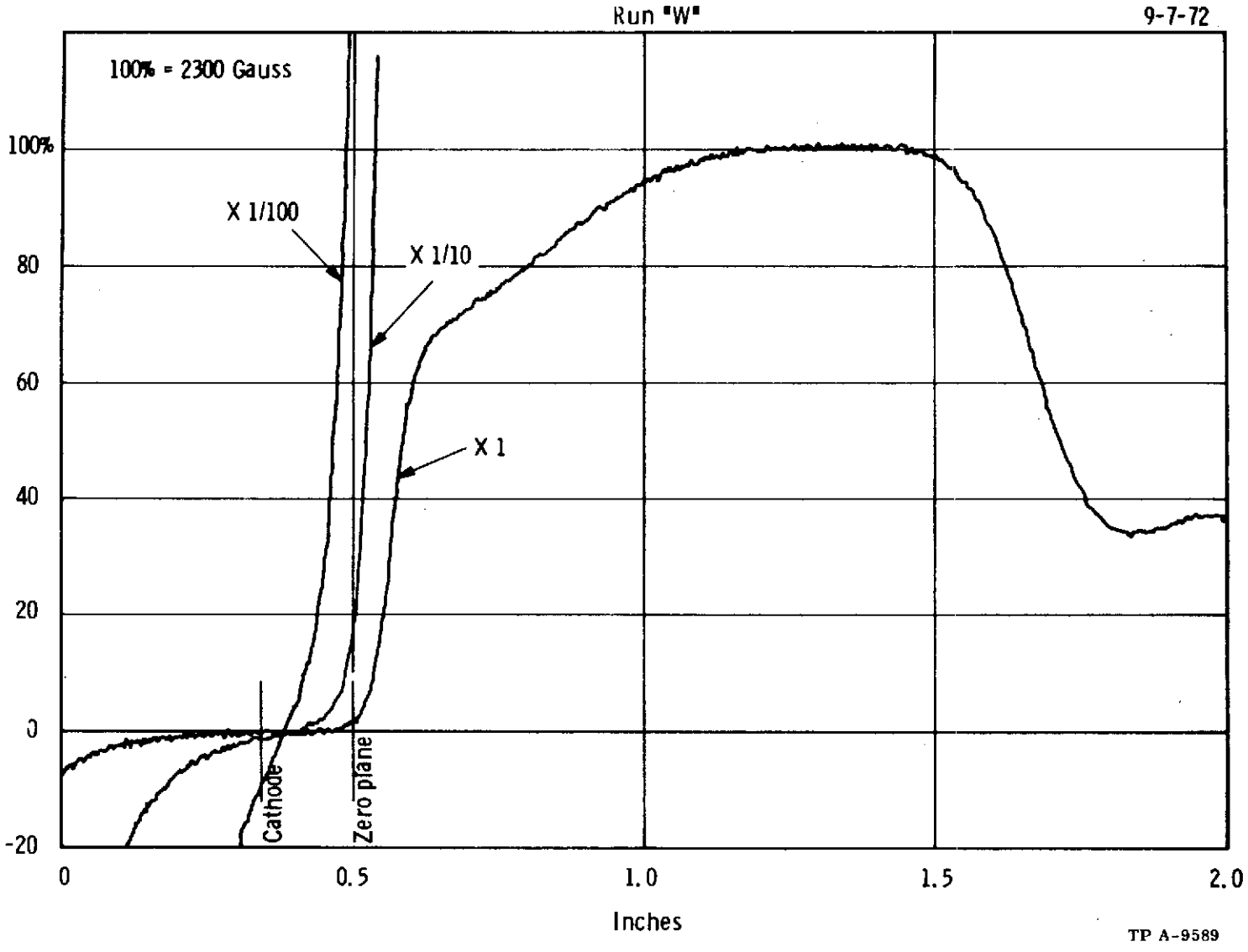

Figure 13. Magnetic Field in the Cathode Region as a Function of Distance

5. MECHANICAL DESIGN

The mechanical design of the VKX-7794 resembles that of many other Varian klystrons at this general frequency range. The major departures from conventional design are brought about by the requirement that this tube must be operable inside a space-simulating vacuum chamber. A removable collector must be provided which can be replaced by a multistage depressed collector for efficiency enhancement studies.

The electron gun is also required to be demountable so that it may be replaced at end of life.

The focusing magnet assembly is also unusual in that it must withstand bakeout at high temperature so that the system may be evacuated to the pressure levels appropriate to klystron operation.

Figure 14 shows the layout drawing with the tube mounted in the permanent magnet focusing assembly. Figure 15 shows a photograph of the tube and magnet assembly.

5.1 RF BODY CONSTRUCTION

The buncher cavities are milled from a solid copper block with thin Monel-backed copper diaphragms brazed into the open ends. The diaphragms are connected to a tuner mechanism for final trim tuning during hot test.

Water cooling of the body block is accomplished through a series of transverse cooling passages drilled through the web between cavities. A heavy copper block is brazed to the body between the input and output waveguides. If possible, a heat pipe is to be attached to this block to conduct away the heat dissipated in the body. In the latter case, direct water cooling of the body will not be necessary.

The input coupling is by way of WR-90 waveguide through a pillbox-type ceramic window, through a tapered transition to half-height waveguide, and through appropriate waveguide bends terminating at the input coupling iris. The output coupling is by way of WR-90 waveguide through a pillbox-type ceramic window, through a full-height waveguide to the filter loaded output cavity.

The gun and collector polepieces are made of soft iron and brazed to the body assembly, and are sized to mate snugly with the magnet polepieces, thereby completing the magnetic circuit.

ORIGINAL PAGE IS
OF POOR QUALITY

REVISIONS				
ZONE	LTR	DESCRIPTION	EO	DATE	APPROVED
	B	UPDATED		2-23-73	

UNLESS OTHERWISE SPECIFIED DIMENSIONS ARE IN INCHES	CONTRACT NUMBER	varian
DECIMALS .XX ± .03 .XXX ± .010	DR VKK 8-11-72	VKK-7794/B KLYSTRON LAYOUT
ANG ± MATERIAL	CHK	
NEXT ASSEMBLY / USED ON / APPLICATION	APPD	SIZE E — CODE IDENT NO. — DWG NO. 055271 — REV B
	APPD	SCALE 2:1 — SHEET OF

Figure 14. Klystron and Focusing Magnet Assembly Layout Drawing

FOLDOUT FRAME 1

FOLDOUT FRAME 2

PRECEDING PAGE BLANK NOT FILMED

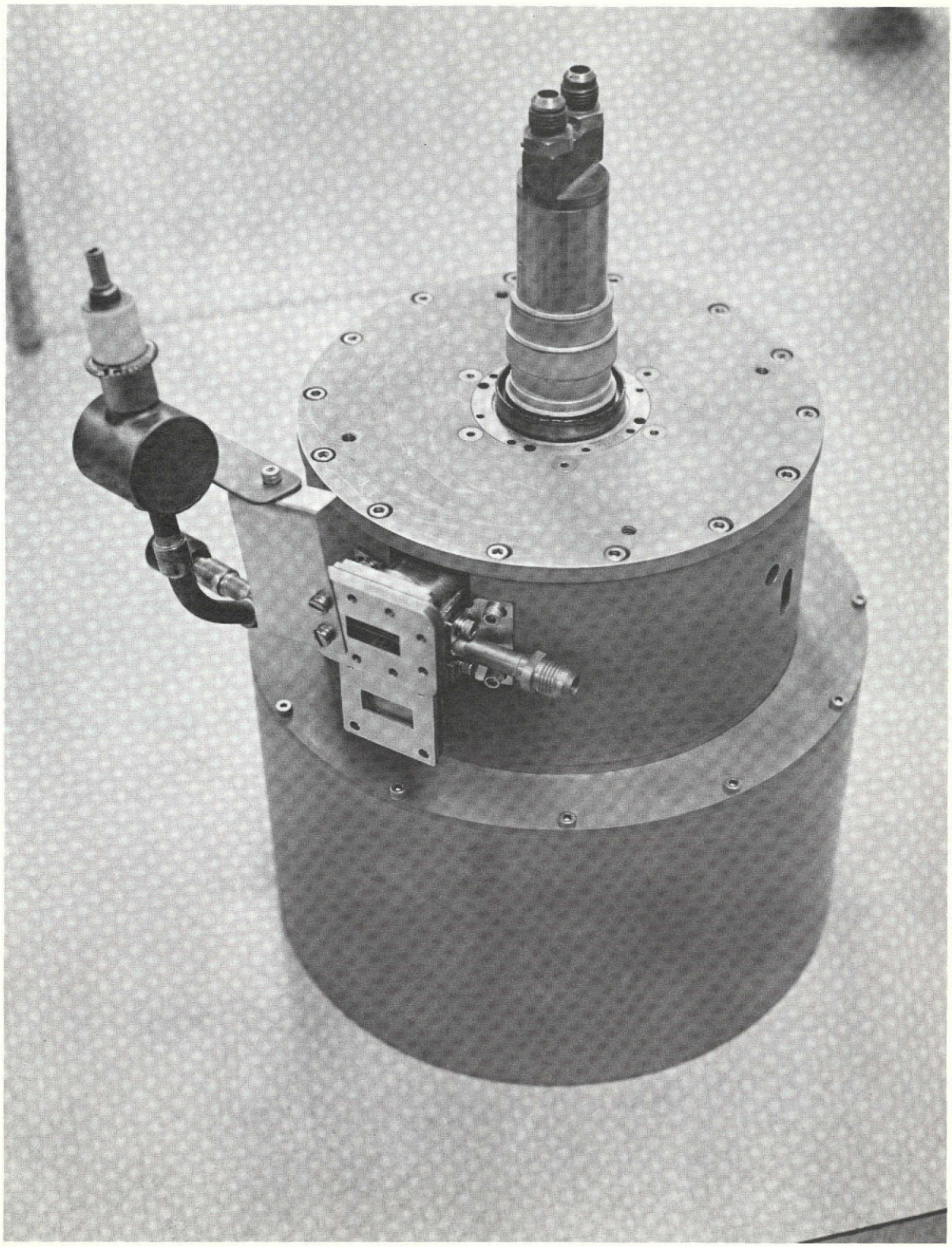

Figure 15. Klystron and Focusing Magnet Assembly

5.2 RF WINDOWS

The input and output waveguide windows consist of thin disc ceramics mounted in circular waveguide, which is an existing design used on a 4 kW cw klystron. The VSWR is less than 1.1:1 across the operating band.

5.3 COLLECTOR

The collector is of conventional design, taken from a 10 kW klystron. It is supported by a ceramic insulator in order to allow for the measurement of beam transmission. The major feature of the collector design is the heliarc flange by which it is mounted to the collector polepiece. This is designed to allow maximum unimpeded access to the beam exit tunnel upon removal of the collector.

5.4 ELECTRON GUN CONSTRUCTION

Figure 16 shows the demountable electron gun. The gun ceramic support cylinder is made large in order to minimize leakage. The cathode employed is a dispenser-type cathode, because an oxide-coated cathode could not be expected to provide the cathode current density required in this application. The cathode is supported by a conical sleeve which is attached to the inside of the focus electrode support sleeve. This assembly is brazed to a heavy support ring attached to the base of the gun ceramic by means of six machine screws.

The original gun vacuum envelope is completed by a secondary feedthrough structure that is heliarc welded to a sleeve at the base of the gun ceramic and to the heater feedthrough rod. At the time of gun replacement, these heliarc joints are cut and the secondary feedthrough plate discarded. The new gun is then mounted in place of the old gun, using the machine screws.

5.5 PERMANENT MAGNET CONSTRUCTION

The permanent magnet assembly consists of a total of 52 segments of samarium-cobalt magnets as shown in Figure 17. Each of the two rings shown consists of 26 segments which are magnetized before assembly. The rings are placed on top of each other, then clamped into the iron cylinder with stainless steel plates.

The floating polepiece is attached to the tube body downstream from the output cavity.

5.6 FILTER-LOADED OUTPUT CIRCUIT

The filter-loaded output circuit consists of a conventional klystron output cavity which, in turn, is iris-coupled to the output waveguide.

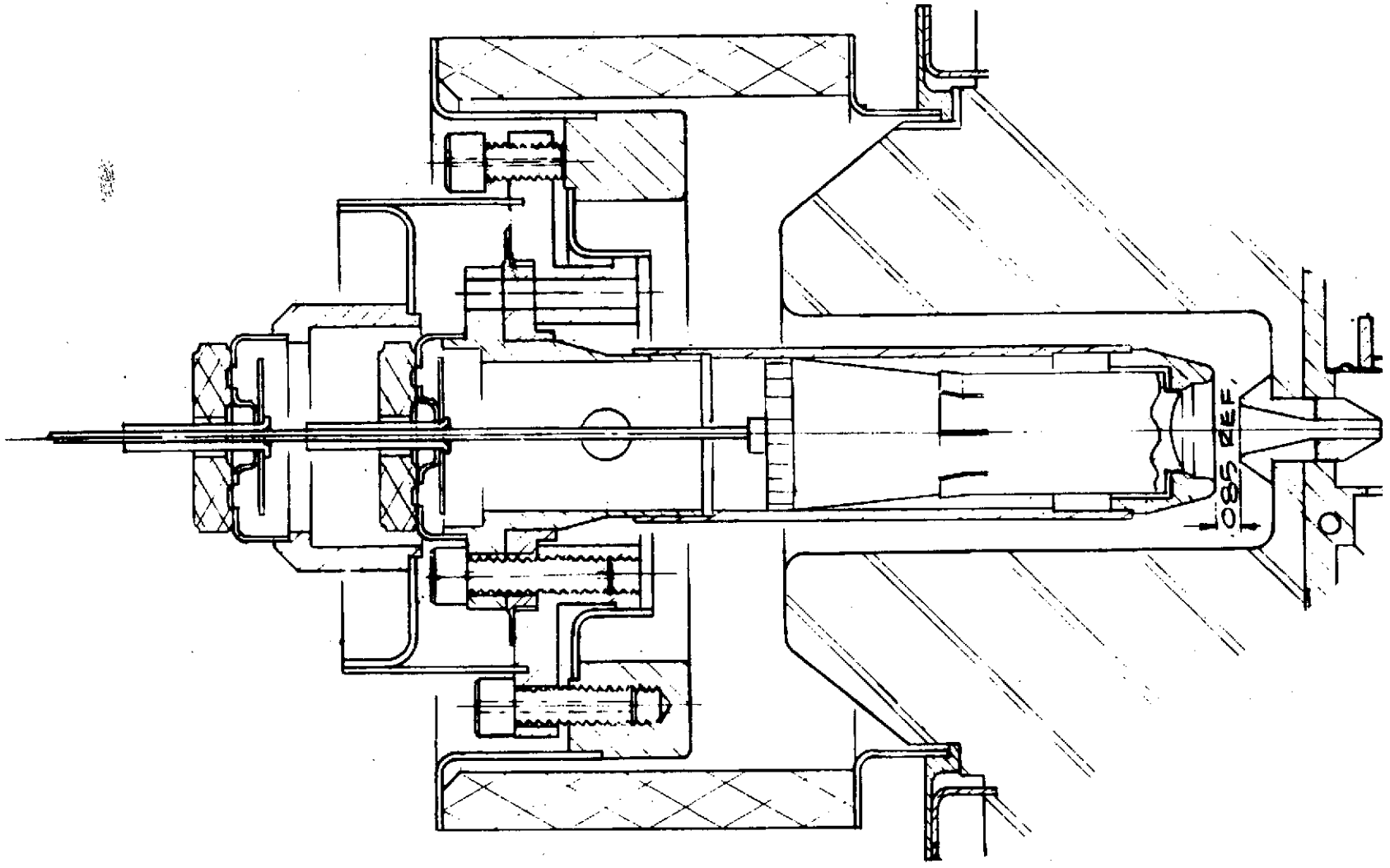

Figure 16. Demountable Electron Gun

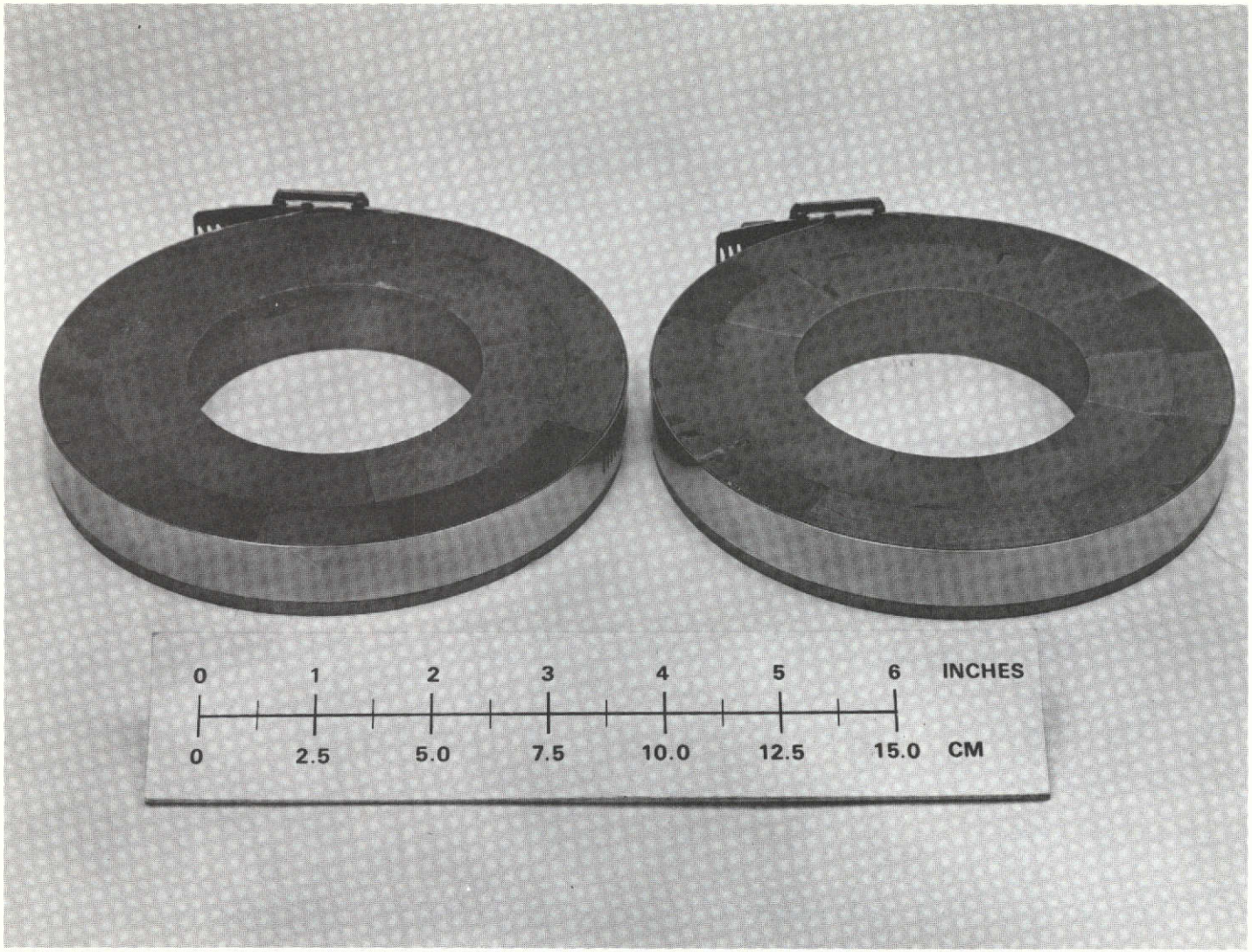

Figure 17. Samarium-Cobalt Magnet

Figure 18 shows the filter-loaded output circuit. Figure 19 shows the real part of the gap impedance as a function of frequency. The graph shows that the maximum circuit impedance is 16,000 ohms instead of the desired 18,400 ohms. This will result in slight over-coupling to the beam and may reduce the efficiency a slight amount. The bandwidth is 40 MHz for the lower channel and 49 MHz for the upper channel. The required bandwidth is 40 MHz for each channel.

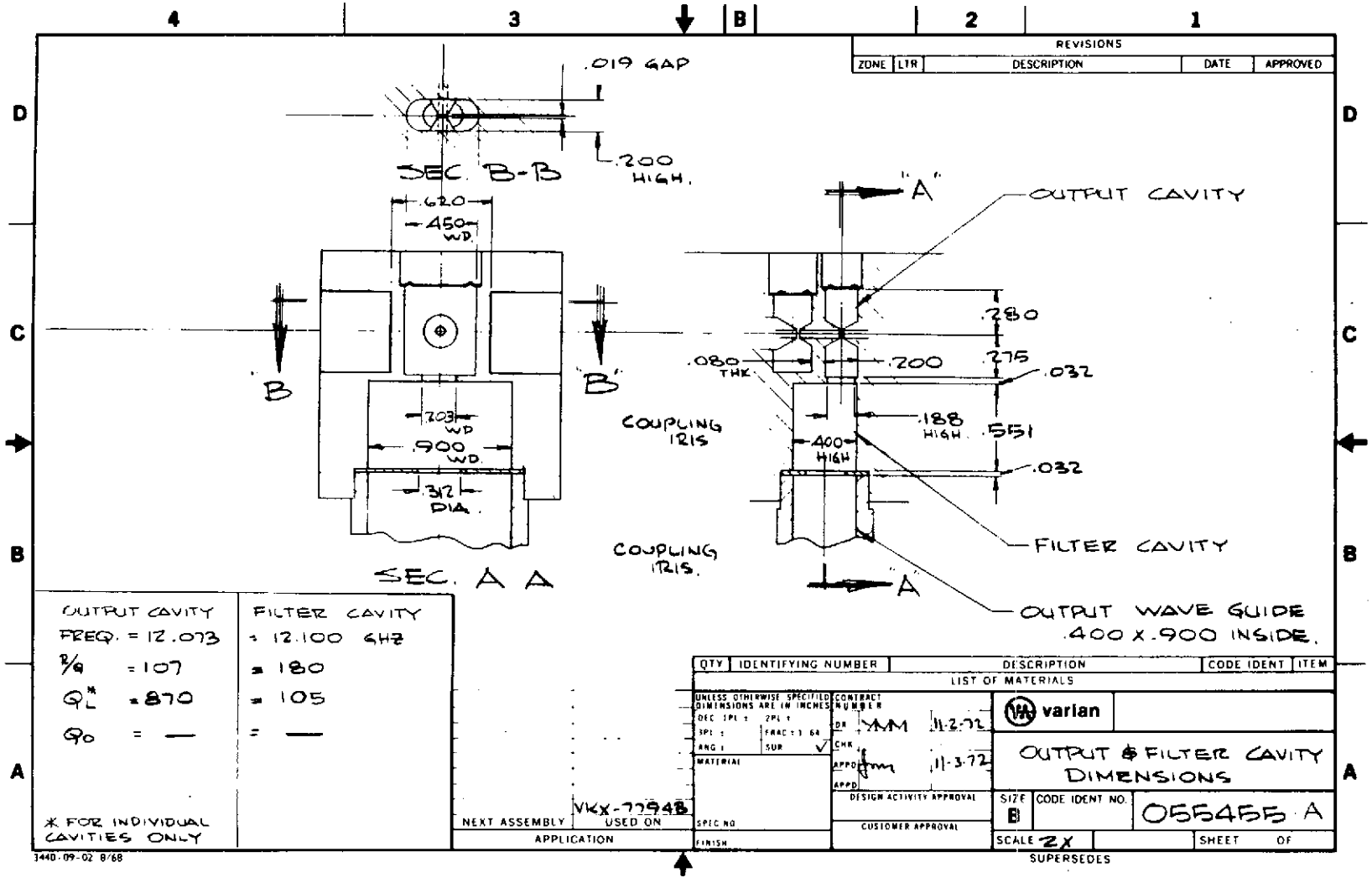

Figure 18. Filter-Loaded Output Circuit

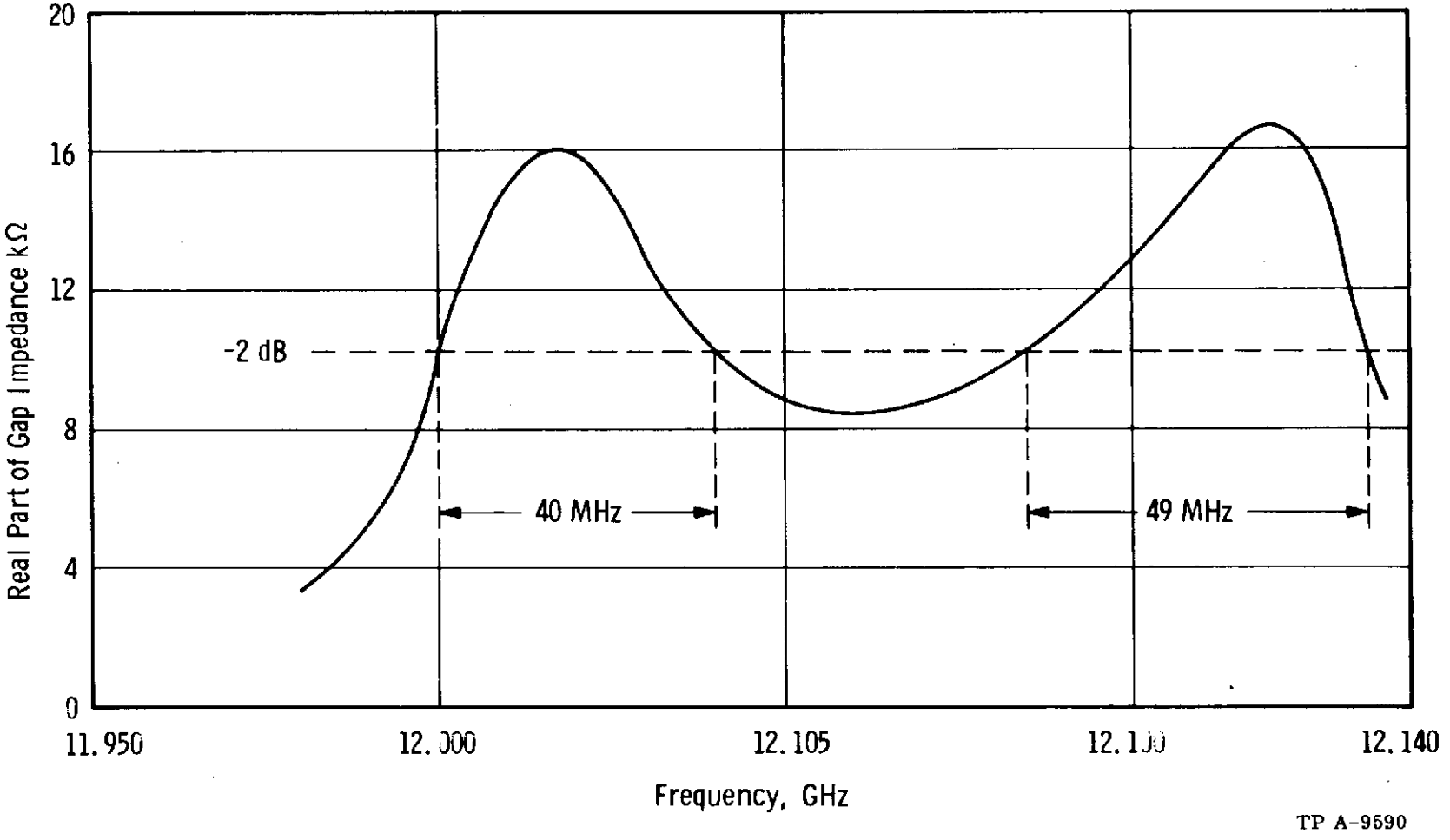

Figure 19. Output Cavity Gap Impedance as a Function of Frequency

6. EXPERIMENTAL RESULTS

6.1 COLD TEST RESULTS

The preliminary cold test work required for selection of cavity dimensions was done on individually-machined copper test sections. Several existing Varian klystrons at similar operating frequencies use the milled-cavity approach, where cavities with full-radius sidewalls are milled into a solid copper block. A beam hole is drilled and the drift tubes are brazed in. This technique has the advantage of being simple and precise, and results in a good thermal design.

The tunnel diameter and drift tube gaps were determined in the analytical design phase of the program, and the cold-test design work was aimed at achieving a cavity size that had the proper resonant frequency, good form factor and maximum R/Q.

Using quartz rod perturbation techniques, the measured R/Q of the first three cavities is 124 ohms and the Q_o is 2800.

The coupling iris for the input cavity is also machined into the copper body block, with the dimension of the coupling iris determined by the desired external Q of 225. Since the presence of the coupling iris also detunes the cavity resonant frequency, an adjustment in cavity length is made to re-establish the desired frequency.

The short drift length desired between the penultimate cavity and the output cavity places a limitation on the length of the downstream drift tube tip. Since the cavity and drift tube size used on the first three cavities would cause the drift length to be too great for good efficiency performance, the gap in the penultimate cavity was moved off center toward the output cavity. This, in turn, lowered the resonant frequency of the cavity to a point where the cavity height had to be reduced (to 0.635 cm) to obtain the desired operating frequency, which in turn lowered the cavity R/Q to 105.

To maximize efficiency, the output cavity has a shorter output gap (0.7 radian) than the driver cavities. This shorter gap and the presence of the output coupling iris lowers the resonant frequency; therefore, the cavity height is reduced to 0.508 cm to compensate for this. The gap is centered in the cavity and the R/Q is 105.

A copper diaphragm end-wall trim tuner is used on all cavities to provide approximately ± 100 MHz tuning with a diaphragm movement of ± 0.05 cm.

The second and third cavities have a small iris coupled to a circular waveguide that contains a lossy silicone-carbide loaded ceramic pellet to provide for external loading. This is necessary to increase the driver section bandwidth to cover the required 120 MHz. The amount of loading is determined from the small signal gain bandwidth program. The position of the pellets is adjustable so the loading may be changed during rf testing.

6.2 EXPERIMENTAL TUBE RESULTS

One tube was fabricated to determine the adequacy of the design. Table IV lists the test results for the experimental tube.

TABLE IV

SERIAL NO. 1 TEST RESULTS

Auxiliary Solenoid Current	0	10 A	0	0
Duty Factor	0.1	0.1	1.0	1.0
Beam Voltage	8 kV	8	6	5
Beam Current	0.54 A	0.54	0.35	0.25
Body Current, avg	52 mA	35	30.5	9
Body Current, peak	170 ma	154	--	--
Body Current without rf	40 mA	24	9.5	5
Power Output, peak	1600 W	1830	520	255
Efficiency	37%	42.3	24.8	20.4
Power Gain	40 dB	41	34	26

Rf operation of the tube at beam voltages over 6 kV results in excessive body current which, in turn, causes thermal detuning of the cavities. In order to get performance data over 6 kV, the tube was operated at a 10% duty cycle. This is done by pulsing the rf drive.

At a beam voltage of 7 kV, power output is 1600 watts peak and efficiency is 37%. The peak body current is 170 ma, which is a beam transmission of 68.5%. The body current without rf is 40 ma for a beam transmission of 93%.

An attempt was made to improve the beam transmission by placing an auxiliary solenoid around the gun. The principal effect of this coil is to increase the magnetic field strength in the main focusing field.

Increasing the solenoid current reduces the body current and increases power output. The power output is increased because reducing the beam interception on the output drift tube results in less thermal detuning. With 10 amperes in the solenoid, the power output increases to 1830 watts peak, the efficiency is 42.3%, and the beam transmission is 72% with rf and 95.6% without rf.

The test results show that a Brillouin-focused beam cannot maintain good beam transmission under rf conditions. With 10 amperes in the auxiliary solenoid the field at the last interaction gap is 1.8 times the Brillouin field and indications are that more field is desirable — which is approaching confined-flow operation.

The best cw operation without the auxiliary coil is at a beam voltage of 5 kV; that is, with reasonable beam transmission and without thermal drift. This corresponds to a field of 2.03 times Brillouin at the last interaction gap. This indicates that in order to operate satisfactorily at 8 kV the focusing field must be increased by at least 40%. The weight of the samarium-cobalt magnet would increase by a factor of two.

7. CONCLUSIONS

An experimental program has been undertaken to demonstrate the feasibility of techniques for achieving 45% conversion efficiency in a samarium-cobalt permanent magnet, Brillouin focused, 2 kW cw klystron operating at 12.045 GHz.

One tube was built to determine the feasibility of the design approach taken.

After determining the value of the focusing field and choosing its shape, a computer program was used to determine the necessary size and shape of the focusing structure. Magnetic field measurements made on the computer-designed circuit show good agreement with the computed design. The limitation of this program is that the permanent magnet must be cylindrically symmetric.

The poor beam transmission under rf conditions has made it extremely difficult to extract meaningful data. Thermal detuning of the penultimate and output cavities causes changes in bandpass characteristics, power output and gain.

Also since a large portion of the beam current does not traverse the output gap, the cavity parameters are not the same as the design parameters, resulting in poor rf performance.

The best performance is achieved by using an auxiliary solenoid to increase the focusing field to near confined-flow condition.

The program has shown that in order to achieve high efficiency and high cw power at 12.0 GHz, it is necessary to use confined-flow focusing to contain the beam during rf operation.

REFERENCES

1. Kavanagh, Francis E., Alexovich, Robert E., and Chomos, Gerald J.: Evaluation of Novel Depressed Collector for Linear-Beam Microwave Tubes. NASA TM X-2322, 1971.

2. Kosmahl, Henry G., A Novel, Axisymmetric, Electrostatic Collector for Linear Beam Microwave Tubes. NASA TN D-6093, 1971.

3. Lien, E. L.: Large-Signal Analysis of Klystrons. International Electron Devices Meeting, Washington, D.C., October 1968.

4. Lien, E. L. : High Efficiency Klystron Amplifiers. Eighth International Conference on Microwave and Optical Generation and Amplification, Amsterdam, Sept. 1970, Section II, pp. 21 - 27.

APPENDIX A

BEAM ANALYZER

A beam analyzer for the evaluation of electron guns is used for this program. Salient features of this machine include a pinhole and split collector arrangement which can be used to scan the beam in two transverse directions as well as along the beam axis, a well-shielded solenoid so that measurements can be made with an applied focusing field, and an oil-free vacuum chamber. A photograph of the unit, together with some auxiliary equipment, is shown in Figure 20. A drawing of the beam analyzer is shown in Figure 21. The following description will be made with reference to these figures.

1. MECHANICAL AND ELECTRICAL DESIGN

The machine is mounted on an angle-iron frame, the top plate of which serves as the bottom of the magnetic shield assembly. The magnetic circuit is a complete shell so that field uniformity in the beam region is assured. The solenoid is provided so that the analysis of a beam can be made in the presence of the confining magnetic field, duplicating conditions as they will exist in the operating tube. The top plate of the magnetic shell, by means of an overlapping joint, supports the mounting flange of the vacuum chamber itself. This mounting flange is also magnetic and is continued into the vacuum chamber without a gap so that the magnetic-field shaping in the gun region of the chamber may be accomplished. Thus, the magnetic aperture at the anode of the gun can be adjusted up to a maximum diameter of 5 inches so that the magnetic leakage field at the cathode can be controlled. Re-entrant magnetic polepieces for shaping of the magnetic field in the gun region can be easily installed.

The vacuum chamber itself is fabricated of stainless steel and is divided by the magnetic mounting flange into two regions: the gun region, which is some 11 inches in diameter and which can be identified in the figures as the cylindrical section just above the large solenoidal housing; and the collector region. The gun chamber is large enough so that guns of substantial size can be mounted within it. The gun chamber has three high-voltage vacuum bushings so that the gun can be cathode-pulsed to 25 kV. A viewport is also provided at about the cathode location, and a multi-pin header is available for thermocouple leads.

The collector, or target region of the analyzer is enclosed by a length of stainless-steel tubing, 6 inches in diameter, and extends downward through a hole in the bottom end of the solenoid assembly. To the lower end of the collector chamber are affixed the mechanical devices necessary to position the target used for scanning the electron beam. The motion is transmitted through the vacuum wall by means of a

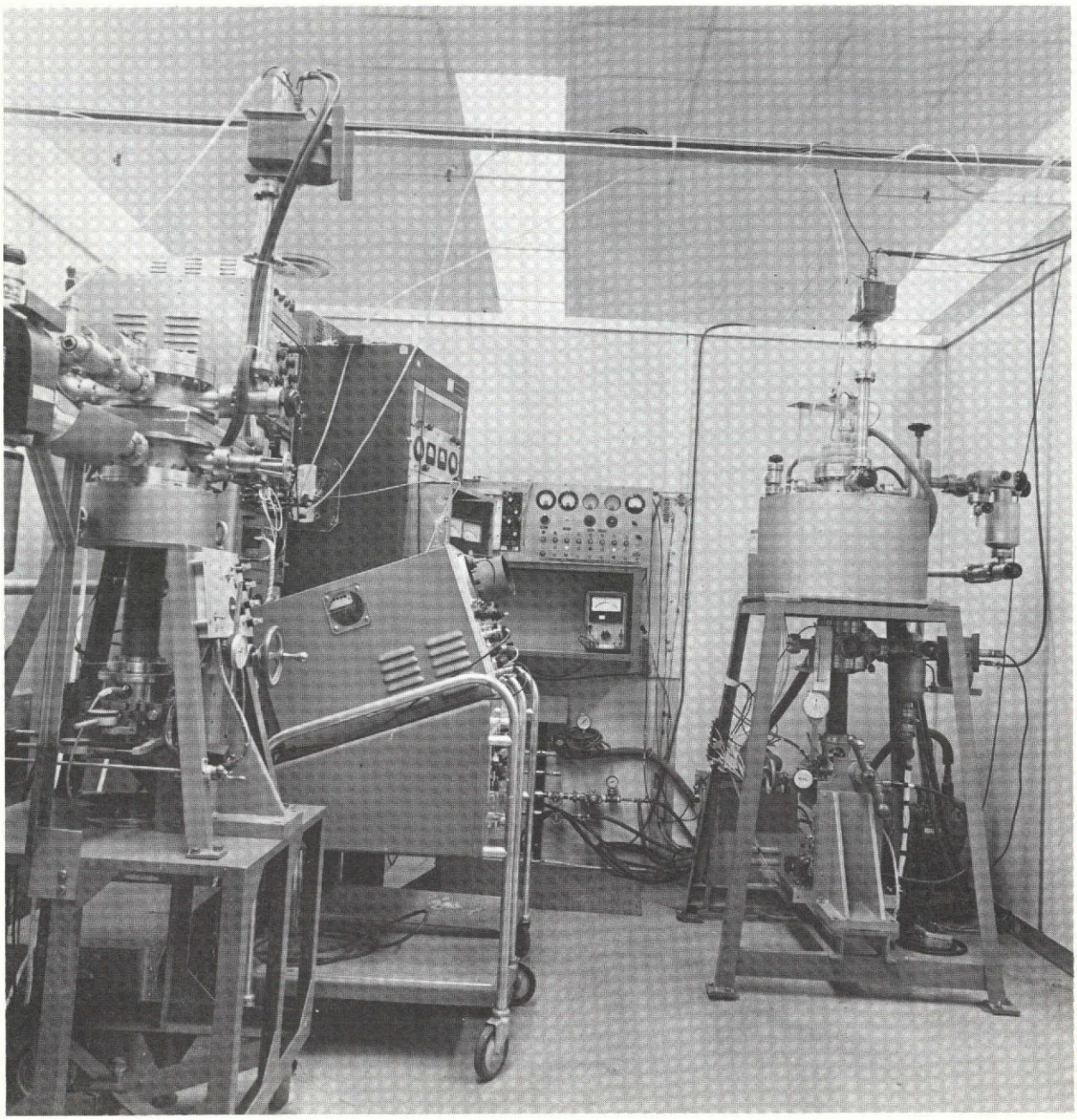

Figure 20. Beam Analyzer and Auxiliary Equipment

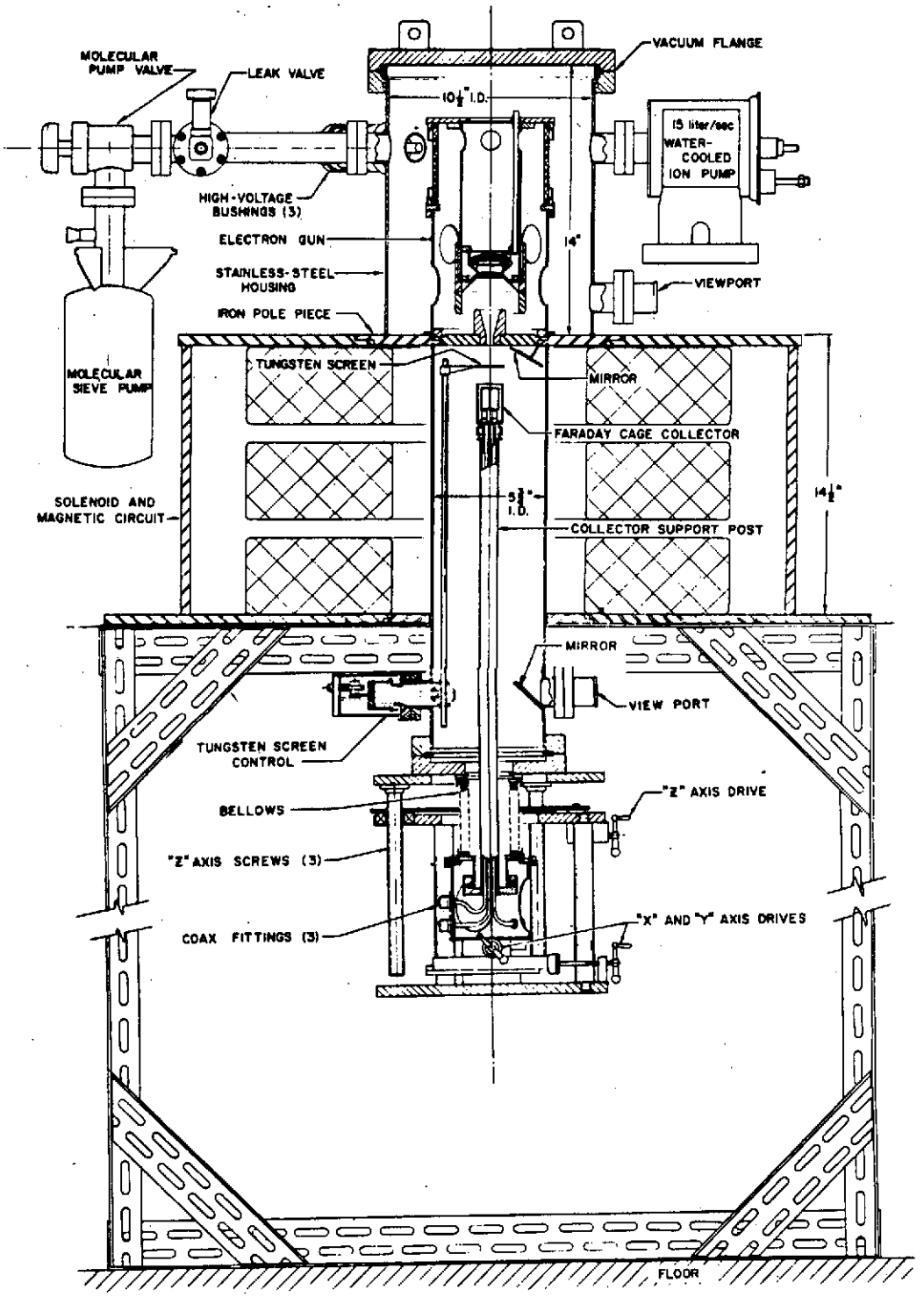

Figure 21. Outline Drawing of the Beam Analyzer

bellows which allows some 8 inches of axial motion, and about 1 inch of motion in either of the two transverse directions. Changes in the transverse position of the collector assembly can be within 0.001 inch. A motor drive for both transverse axes is used in combination with a recorder for automatic plotting of the output from the collector.

Electrical observations of the beam are made with the use of a Faraday-cage collector assembly. This assembly consists of a shielded split-collector located behind an apertured molybdenum target which intercepts the major portion of the beam. By moving this pinhole collector throughout the beam, the current density distribution in the beam may be established. In addition, the division of current to the two halves of the split collector is a measure of the transverse velocity distribution in the beam.

For visual observation of the beam, a tungsten mesh target can be rotated into the beam. The beam image is reflected, by a system of two mirrors, through a viewport located at the bottom end of the chamber. A telescope located at this port makes possible a visual check on the beam size and shape under the influence of changing potentials and magnetic fields. The same telescope is used for pyrometric measurements of the cathode temperature.

The pulses from the modulator used during tests of the gun are synchronized to zero ac heater current in order to eliminate the effect of the magnetic field produced by the heater. Provisions are made for demagnetization of the solenoid frame to create a predictable magnetic flux density in the gun region.

APPENDIX B

LIST OF SYMBOLS

a	drift tube inner radius
b	beam radius
c	free-space velocity of light
E_b	dc beam voltage
E_f	heater voltage
I_b	dc beam current
I_{by}	body current
I_f	heater current
Imag	focusing solenoid current
ℓ	axial length
M	cavity gap coupling coefficient
P_d	rf drive power
P_o	output power
Q	quality factor of resonant cavity
Q_o	unloaded Q
Q_e	external Q
Q_L	total loaded Q
R/Q, R_{sh}	cavity interaction gap shunt resistance
u_o	dc beam velocity
V_o	dc beam voltage
VSWR	voltage standing wave ratio
β_e	propagation factor associated with the dc beam velocity ($\beta_e = \omega/u_o$)
β_q	plasma propagation factor ($\beta_q = \omega q/u_o$)
γ	relativistic propagation factor $\left(r = \beta_e \left[1 - (u_o/c)^2\right]^{1/2}\right)$
η	conversion efficiency

ϕ	rf phase shift
ω	angular frequency
ωq	reduced plasma angular frequency
B	magnetic field in gauss

DISTRIBUTION LIST

NASA CR-134761
February 1975

NATIONAL AERONAUTICS AND SPACE ADMINISTRATION

Headquarters
Washington, D.C. 20546
Attention: SC/Dr. R. B. Marsten
REM/E. C. Buckley

NASA-Lewis Research Center
21000 Brookpark Road
Cleveland, Ohio 44135
Attention: H. W. Plohr (MS 54-1)
R. E. Alexovich (MS 54-5)
F. E. Kavanagh (MS 54-5)
Dr. H. G. Kosmahl (MS 54-5)
Technical Utilization Off. (MS 3-19)
Contracts Section B

A. J. Doskocil (MS 54-1)
Audit Branch (MS 500-303)

NASA-George C. Marshall Space Flight Center
Huntsville, Alabama 35812
Attention: E. C. Hamilton (RASRT-A)

General Electric Company
Tube Department
Microwave Tube Operations
Schenectady, NY. 12305
Attention: Mr. D. Hawkins

Jet Propulsion Laboratory
4800 Oak Grove Drive
Pasadena, California 91103
Attention: L. Derr

Litton Industries
Tube Division
960 Industrial Road
San Carlos, California 94070
Attention: Larry Jones

Dr. G. Haas
Office of Naval Research
Defense Department
Washington, D.C. 20390

NASA Scientific and Technical
Information Facility
Attention: Acquisitions Branch
P. O. Box 33
College Park, Maryland 20740 (2)

Hughes Aircraft Company
Electron Dynamics Division
P. O. Box 2999
Torrance, California 90509
Attention: Mr. M. Kreismanis

Mr. E. Lien
Varian Associates
611 Hansen Way
Palo Alto, California 94304

D. F. Barber
Chief Reliability Branch
Dept. of the Air Force
Griffiss AFB, New York 13440

Dr. L. Lesensky
Raytheon Company
Waltham, Mass. 02154

Dr. E. S. Rittner
Comsat Laboratories
Clarksburg, Maryland 20743

National Technical Information Service
Springfield, Virginia 22151 (40)